An Anisotropic Material Model for Finite Rubber Viscoelasticity

D. Liefeith[1], S. Kolling[2]

[1] DaimlerChrysler AG, EP/SPB, HPC X271, 71059 Sindelfingen
Email: Stefan.Kolling@DaimlerChrysler.com

[2] DaimlerChrysler AG, EP/SPB, HPC X271, 71059 Sindelfingen
Email: Dirk.Liefeith@DaimlerChrysler.com

Abstract:

In this article a formulation of an anisotropic finite linear viscoelasticity model is proposed. In particular, transverse isotropy and orthotropy is considered. The aim of this work is to establish a material model, which allows the description of an anisotropic material response in the framework of the finite deformation theory. First of all, the fundamentals of finite hyperelasticity are discussed. In the next step, we consider a finite linear viscoelastic formulation which is then extended to the theory of anisotropy. After giving an introduction to the coordinate free representation of anisotropic material behaviour using isotropic tensor functions in terms of structural tensors, we derive the constitutive equations for the orthotropic linear viscoelasticity model. This model is implemented into the nonlinear finite element code LS-DYNA. Both, an explicit and an implicit implementation is carried out. To evaluate the performance of the model, representative numerical examples are discussed in detail.

Keywords:

Finite Hyperelasticity; Finite Linear Viscoelasticity; Anisotropy; Structural tensors; Transverse Isotropy; Orthotropy

© 2007 Copyright by DYNA*more* GmbH

1. Introduction

Since rubber-like materials have a wide range of applications, the need for the establishment of constitutive models characterizing highly nonlinear rate-dependent inelastic material behaviour at finite deformations has tremendously increased. It may be observed that it is not only an active subject of the current research, but it is also of great importance in engineering practice. For instance, rubber-like materials are used for modeling soft tissue in the field of biomechanics. They are widely spread in the field of structural mechanics as well. For example, the engine mounts as depicted in Figure 1a are an application in the automotive industry.

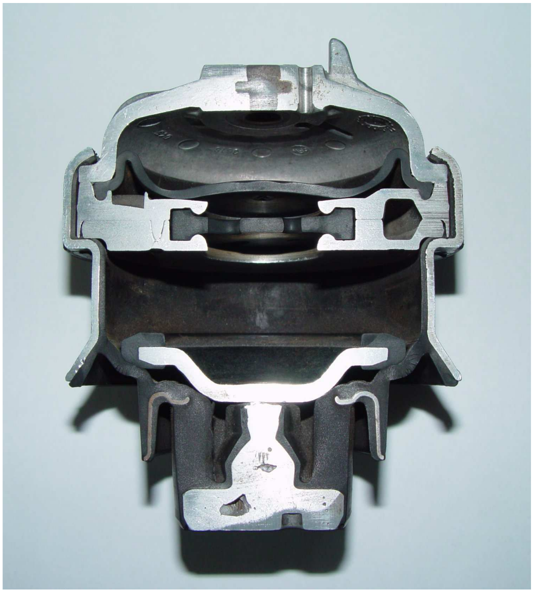

(a)

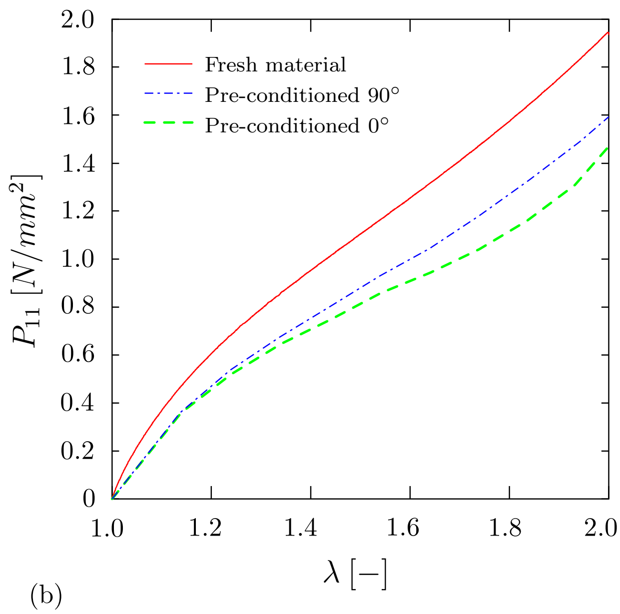

(b)

Figure 1: (a) Sectional view of an engine mount (b) Experiments for particle-filled rubber

The material used in a component like the engine mount is a particle-filled rubber made up of small particles embedded into a softer matrix material. Reinforcement of the rubber matrix by stiff particles enhances the mechanical properties of the material. A side effect of the reinforcement is the phenomenon commonly known as *Mullin's effect*. Recent studies have shown that Mullins-type deformation-induced softening is an anisotropic effect strongly dependent on the deformation history. To this end, we consider a sheet of the material, which was pre-conditioned in one direction up to an elongation of 100%. Afterwards tensile test specimen were cut out in the direction of the pre-conditioning, denoted as 0°, and transverse to this direction, referred to as 90°. Comparison of the nominal tensile stress-stretch curves in Figure 1b indicates a distinct discrepancy between the fresh and the pre-conditioned material specimen. The anisotropic nature of the deformation-induced *Mullin's effect* is clearly observed in the stress curves of the pre-conditioned

 © 2007 Copyright by DYNAmore GmbH

specimens subjected to tension in perpendicular directions. The pre-conditioned material can be classified as anisotropic.

The intent of this work is the construction of a constitutive model, particularly for transversely isotropic and orthotropic viscoelastic materials at finite deformations. For this purpose, we first define a polyconvex isotropic free energy function for a hyperelastic and linear viscoelastic material. Then we continue with the extension of these functions to the theory of anisotropy at finite deformations in the framework of a coordinate free representation using structural tensors. Hence, the anisotropic free energy function is formulated as an isotropic tensor function in terms of the invariants of the argument tensors. In order to define such a function, a set of irreducible invariants, the so-called integrity basis, needs to be derived for a transversely isotropic and orthotropic material, whereas the transverse isotropic intergity basis is included in the orthotropic one.

The outlined model is implemented into LS-DYNA and representative boundary value problems are considered in a finite element analysis reflecting the underlying anisotropic rate-dependent material behaviour at finite deformations.

2. Isotropic Finite Elasticity

2.1. Kinematics at Finite Deformations

Consider a nonlinear deformation $\boldsymbol{\varphi} : \boldsymbol{X} \mapsto \boldsymbol{x} = \boldsymbol{\varphi}(\boldsymbol{X}, t)$ mapping material points $\boldsymbol{X}$ from the reference configuration $\mathcal{B}$ onto points $\boldsymbol{x}$ of the current configuration $\mathcal{S}$. The Frechet-derivative, or directional derivative, of the deformation map $\boldsymbol{\varphi}$ is denoted as the deformation gradient $\boldsymbol{F}$, defined as

$$\boldsymbol{F}(\boldsymbol{X}, t) := D\boldsymbol{\varphi}(\boldsymbol{X}, t) = \frac{\partial \boldsymbol{\varphi}(\boldsymbol{X}, t)}{\partial \boldsymbol{X}} \quad \text{with } J = \det[\boldsymbol{F}] > 0 \,. \tag{1}$$

The deformation gradient $\boldsymbol{F}$ maps tangents $d\boldsymbol{X} \in T_X\mathcal{B}$ to material curves onto tangents $d\boldsymbol{x} \in T_x\,\mathcal{S}$ to deformed curves of the current configuration. $T_X\mathcal{B}$ and $T_x\,\mathcal{S}$ are the tangent spaces of the reference and current configuration. With this picture in mind, $\boldsymbol{F}$ is referred to as the tangent map. Additional mappings for infinitesimal area and volume elements, the normal and volume map, are given by

$$\begin{aligned} d\boldsymbol{a} &= J\boldsymbol{F}^{-T} d\boldsymbol{A} = \operatorname{cof}\,[\boldsymbol{F}]\, d\boldsymbol{A} \\ dv &= J dV \,. \end{aligned} \tag{2}$$

For a more comprehensive discussion of the fundamentals of continuum mechanics, the reader is referred to the literature provided by Marsden & Hughes [8] and Malvern [7].

2.2. Decoupled Volumetric-Isochoric Finite Elasticity

Rubbery polymers exhibit an almost incompressible (infinitely stiff) volumetric response and a very soft isochoric response. As stated in Ogden [10], a material is said to deform isochoricly (volume preserving), if its volume does not change locally during the deformation. The incompressibility condition corresponds to $J = \det[\boldsymbol{F}] = 1$. Owing to the incompressibility condition it is reasonable to introduce quantities characterizing the volumetric and isochoric deformation seperately. In order to achieve that, the multiplicative decomposition

$$\boldsymbol{F} = \boldsymbol{F}^{iso}\boldsymbol{F}^{vol} \tag{3}$$

of the deformation gradient is used. The part $\boldsymbol{F}^{vol}$, which is a spherical tensor accounting for the entire change of volume, then has to be defined according to

$$\boldsymbol{F}^{vol} = J^{\frac{1}{3}}\boldsymbol{1} \,. \tag{4}$$

A similar restriction as for $\boldsymbol{F}^{vol}$ holds for $\boldsymbol{F}^{iso}$ as well, since the isochoric part of $\boldsymbol{F}$ must not contribute to the change of volume, i.e. $\det\left[\boldsymbol{F}^{iso}\right] = 1$. Hence, the isochoric part of the deformation gradient is given by

$$\boldsymbol{F}^{iso} = \boldsymbol{F}(\boldsymbol{F}^{vol})^{-1} = J^{-\frac{1}{3}}\boldsymbol{F} =: \bar{\boldsymbol{F}} \,. \tag{5}$$

The volumetric-isochoric split shall also be considered in the formulation of the free energy function Ψ additivly by

$$\Psi = \Psi^{vol}(J) + \Psi^{iso}(\bar{\boldsymbol{F}}) \,. \tag{6}$$

Motivated from the *principle of material symmetry*, the isochoric part of the free energy function can also be expressed in terms of the right Cauchy-Green tensor $\boldsymbol{C} = \boldsymbol{F}^T\boldsymbol{F}$. The alternative representation of the free energy function Ψ, which we will be used in this work, then reads

$$\Psi = \Psi^{vol}(J) + \Psi^{iso}(\bar{\boldsymbol{C}}) \,. \tag{7}$$

2.3. An Incompressible Material Model for Isotropic Finite Elasticity

Before pointing out the specific forms of the free energy function Ψ used for the different material models, we discuss the *principle of material symmetry* and the *principle of material objectivity*. A comprehensive treatment is beyond the scope of this work. For a more detailed treatment, for example the reader is referred to Malvern [7].

Materials may display inherent symmetries allowing certain rotations of the reference configuration leaving the constitutive response unchanged. This means that for certain transformations $\boldsymbol{Q} \in \mathcal{G}$ of the material, the material structure is mapped onto itself such that no difference is visible in the initial state. The set of the allowed rotations $\mathcal{G} \subset \mathcal{O}(3)$ is called the symmetry group of the material and $\mathcal{O}(3)$ is the orthogonal group with the properties

$$\mathcal{O}(3) := \{\boldsymbol{Q} \in \mathbb{R}^{3\times3} \,|\, \boldsymbol{Q}^T\boldsymbol{Q} = \boldsymbol{1} \quad \text{and} \quad \det[\boldsymbol{Q}] = \pm 1\} \,. \tag{8}$$

Combining the requirement of the *principle of material objectivity* and the *principle of material symmetry*, we arrive at the so-called invariance condition of the reduced form

$$\hat{\Psi}(\boldsymbol{Q}\boldsymbol{C}\boldsymbol{Q}^T) = \hat{\Psi}(\boldsymbol{C}) \qquad \forall\, \boldsymbol{Q} \in \mathcal{G} \,. \tag{9}$$

For the case of isotropy the symmetry group $\mathcal{G}$ of the material is identical to the entire orthogonal group $\mathcal{O}(3)$, i.e.

$$\mathcal{G} \equiv \mathcal{O}(3) \,. \tag{10}$$

© 2007 Copyright by DYNA*more* GmbH

If we restrict ourselves to transformations $\boldsymbol{Q}$ belonging to the special orthogonal group $\mathcal{SO}(3) \subset \mathcal{O}(3)$ with the properties

$$\mathcal{SO}(3) := \{\boldsymbol{Q} \in \mathbb{R}^{3\times 3} \,|\, \boldsymbol{Q}^T\boldsymbol{Q} = \boldsymbol{1} \quad \text{and} \quad \det[\boldsymbol{Q}] = +1\}\,, \tag{11}$$

we end up with

$$\hat{\Psi}(\boldsymbol{QCQ}^T) = \hat{\Psi}(\boldsymbol{C}) \qquad \forall\, \boldsymbol{Q} \in \mathcal{SO}(3)\,. \tag{12}$$

Note that due to the restriction to the special orthogonal group $\mathcal{SO}(3)$ as the symmetry group of the material, it will be sufficient to find an integrity basis for symmetric second-order tensors and vectors, which will be discussed, when considering anisotropy in Section 4.1. It can be shown that together with the spectral representation of the right CAUCHY-GREEN tensor, the isotropy condition (9) may only be satisfied, if the free energy function Ψ does not depend on the principal directions but only on the eigenvalues of $\boldsymbol{F}$. Then, a representation of an isotropic free energy function has the form

$$\Psi = \tilde{\Psi}(\lambda_1, \lambda_2, \lambda_3)\,, \tag{13}$$

where λ_1, λ_2 and λ_3 stand for the principal stretches. Since the principal invariants of the right CAUCHY-GREEN tensor are symmetric functions of the principal stretches

$$\begin{aligned} I_1 &= \operatorname{tr}[\boldsymbol{C}] = \lambda_1^2 + \lambda_2^2 + \lambda_3^2 \\ I_2 &= \frac{1}{2}(\operatorname{tr}[\boldsymbol{C}]^{\,2} - \operatorname{tr}\left[\boldsymbol{C}^2\right]) = \lambda_1^2\lambda_2^2 + \lambda_2^2\lambda_3^2 + \lambda_1^2\lambda_3^2 \\ I_3 &= \det[\boldsymbol{C}] = \lambda_1^2\lambda_2^2\lambda_3^2\,, \end{aligned} \tag{14}$$

we may also constitute an isotropic free energy function Ψ as a function of the invariants of $\boldsymbol{F}$, i.e.

$$\Psi = \hat{\Psi}(I_1, I_2, I_3)\,. \tag{15}$$

Recall that the incompressibility condition requires $J = \det[\boldsymbol{F}] = \sqrt{\det[\boldsymbol{C}]} = 1$, considering the isochoric part $\bar{\boldsymbol{C}}$ of the right CAUCHY-GREEN tensor in the formulation and insertion into (14), we obtain the isochoric invariants

$$\begin{aligned} \bar{I}_1 &= \operatorname{tr}\left[\bar{\boldsymbol{C}}\right] \\ \bar{I}_2 &= \frac{1}{2}(\operatorname{tr}\left[\bar{\boldsymbol{C}}\right]^{\,2} - \operatorname{tr}\left[\bar{\boldsymbol{C}}^2\right]) \qquad (16) \\ \bar{I}_3 &= \det\left[\bar{\boldsymbol{C}}\right] = 1\,. \qquad (17) \end{aligned}$$

Since $\bar{I}_3$ is constant, the free energy function Ψ does not depend on the third invariant and therefore it is sufficient to formulate the free energy

$$\Psi = \hat{\Psi}(\bar{I}_1, \bar{I}_2)\,. \tag{18}$$

Volumetric and Isochoric 2nd Piola-Kirchhoff Stresses

Following Coleman's method, the 2^{nd} PIOLA-KIRCHHOFF stresses are derived from the free energy function according to

$$\boldsymbol{S} = 2\partial_{\boldsymbol{C}}\Psi = 2\partial_{\boldsymbol{C}}(\Psi^{vol} + \Psi^{iso}) = \boldsymbol{S}^{vol} + \boldsymbol{S}^{iso} \,. \tag{19}$$

The isochoric part of the 2^{nd} PIOLA-KIRCHHOFF stress tensor is derived from the free energy function using the chain-rule operation, i.e.

$$\boldsymbol{S}^{iso} = 2\partial_{\boldsymbol{C}}\Psi^{iso} = 2\partial_{\bar{\boldsymbol{C}}}\Psi^{iso} : \partial_{\boldsymbol{C}}\bar{\boldsymbol{C}} = \bar{\boldsymbol{S}}^{iso} : \mathbb{Q} \,, \tag{20}$$

where $\bar{\boldsymbol{S}}^{iso} := 2\partial_{\bar{\boldsymbol{C}}}\Psi^{iso}$ and $\mathbb{Q} = J^{-\frac{2}{3}}\left[\mathbb{I} - \frac{1}{3}\boldsymbol{C}\otimes\boldsymbol{C}^{-1}\right]$. For the derivations of (20) and the upcoming equations we make use of the results

$$\partial_{\boldsymbol{C}} J = \frac{1}{2} J\boldsymbol{C}^{-1} \tag{21}$$

$$\partial_{\boldsymbol{C}}\boldsymbol{C} = \mathbb{I} \,, \quad \{\mathbb{I}\}_{ijkl} := \frac{1}{2}\left[\delta_{ik}\delta_{jl} + \delta_{il}\delta_{jk}\right] \tag{22}$$

$$\partial_{\boldsymbol{C}}\boldsymbol{C}^{-1} = -\mathbb{I}_{\boldsymbol{C}^{-1}} \,, \quad \{\mathbb{I}_{\boldsymbol{C}^{-1}}\}_{ijkl} := \frac{1}{2}\left[C^{-1}_{ik}C^{-1}_{jl} + C^{-1}_{il}C^{-1}_{jk}\right] \,. \tag{23}$$

In order to calculate the isochoric chain-rule stresses $\bar{\boldsymbol{S}}^{iso}$, we claim a free energy function being expressed in the first and second principal invariants $\bar{I}_1$ and $\bar{I}_2$. We obtain the expression

$$\bar{\boldsymbol{S}}^{iso} = 2\,\partial_{\bar{\boldsymbol{C}}}\hat{\Psi}^{iso}(\bar{I}_1,\bar{I}_2) = 2\,(\partial_{\bar{I}_1}\hat{\Psi}^{iso}\,\partial_{\bar{\boldsymbol{C}}}\bar{I}_1 + \partial_{\bar{I}_2}\hat{\Psi}^{iso}\,\partial_{\bar{\boldsymbol{C}}}\bar{I}_2) \,. \tag{24}$$

Together with the derivatives of the invariants $\bar{I}_1$ and $\bar{I}_2$ with respect to $\bar{\boldsymbol{C}}$

$$\partial_{\bar{\boldsymbol{C}}}\bar{I}_1 = \boldsymbol{1} \quad \text{and} \quad \partial_{\bar{\boldsymbol{C}}}\bar{I}_2 = (\bar{I}_1\boldsymbol{1} - \bar{\boldsymbol{C}}) \,, \tag{25}$$

we obtain the general expression for the chain rule 2^{nd} PIOLA-KIRCHHOFF stresses, i.e.

$$\boxed{\bar{\boldsymbol{S}}^{iso} = 2\left[\partial_{\bar{I}_1}\hat{\Psi}^{iso}\,\boldsymbol{1} + \partial_{\bar{I}_2}\hat{\Psi}^{iso}\,(\bar{I}_1\boldsymbol{1} - \bar{\boldsymbol{C}})\right]} \tag{26}$$

Owing to the fairly good fitting performance of the hyperelasticity model proposed by YEOH [21] in comparison with the benchmark data provided by TRELOAR [19], we use the free energy function

$$\Psi^{iso} = \hat{\psi}^{iso}(\bar{I}_1) = C_{10}(\bar{I}_1 - 3) + C_{20}(\bar{I}_1 - 3)^2 + C_{30}(\bar{I}_1 - 3)^3 \tag{27}$$

for the isotropic elastic contribution. Together with (26) and the derivatives (25), we arrive at

$$\bar{\boldsymbol{S}}^{iso} = 2\left[C_{10} + 2C_{20}(\bar{I}_1 - 3) + 3C_{30}(\bar{I}_1 - 3)^2\right]\boldsymbol{1} \,. \tag{28}$$

 © 2007 Copyright by DYNA*more* GmbH

To complete the equation for the stresses, we need to define the volumetric part of the 2^{nd} PIOLA-KIRCHHOFF stresses

$$\boldsymbol{S}^{vol} = 2\partial_{\boldsymbol{C}}\Psi^{vol}(J) = 2\underbrace{\partial_J\Psi^{vol}}_{\Psi^{vol'}}\,\partial_{\boldsymbol{C}}J \overset{(21)}{=} \underbrace{J\Psi^{vol'}}_{=:p}\,\boldsymbol{C}^{-1}\,. \tag{29}$$

The quantity p in equation (29) is denoted as the hydrostatic pressure. The hydrostatic pressure is derived from the penalty function $\Psi^{vol}(J)$, which is necessary in order to ensure incompressibility in a numerical framework. Various definitions of such penalty functions may be extracted from the literature provided by SIMO & TAYLOR [15] or MIEHE [9] among others.

Volumetric and Isochoric Lagrangian Moduli

When deriving a formulation, which may also be implemented into an implicit finite element code, the derivation of the moduli is inevitable. The sensitivity of the stresses to the deformation for nonlinear elastic materials is characterized by the rate expression

$$\dot{\boldsymbol{S}} = \mathbb{C} : \frac{1}{2}\,\dot{\boldsymbol{C}}\,, \tag{30}$$

where the fourth order tensor $\mathbb{C}$ represents the Lagrangian moduli. They are obtained by comparing the time derivative of $\boldsymbol{S}$ to the rate expression stated above.

$$\begin{aligned} \boldsymbol{S} &= 2\partial_{\boldsymbol{C}}\Psi \\ \dot{\boldsymbol{S}} &= 2\partial^2_{\boldsymbol{CC}}\Psi : \dot{\boldsymbol{C}} = 4\partial^2_{\boldsymbol{CC}}\Psi : \frac{1}{2}\dot{\boldsymbol{C}} \end{aligned} \tag{31}$$

Hence, the Lagrangian moduli are identified as

$$\mathbb{C} := 4\partial^2_{\boldsymbol{CC}}\Psi\,. \tag{32}$$

In the first step of the derivation of the additive representation of the Lagrangian moduli

$$\mathbb{C} = \mathbb{C}^{vol} + \mathbb{C}^{iso}\,, \tag{33}$$

we consider the isochoric contribution $\mathbb{C}^{iso}$, i.e.

$$\begin{aligned} \mathbb{C}^{iso} &:= 4\partial^2_{\boldsymbol{CC}}\Psi^{iso}(\bar{\boldsymbol{C}}) \overset{(20)}{=} 2\partial_{\boldsymbol{C}}(\bar{\boldsymbol{S}}^{iso} : \mathbb{Q}) \\ &= \mathbb{Q}^T : \bar{\mathbb{C}}^{iso} : \mathbb{Q} + \bar{\boldsymbol{S}}^{iso} : \mathbb{M} \end{aligned} \tag{34}$$

introducing $(\mathbb{Q}_{mnij})^T = \mathbb{Q}_{ijmn}$. In equation (34) we defined the sixth-order tensor $\mathbb{M}$

$$\mathbb{M} = \frac{2}{3}J^{-\frac{2}{3}}\left\{\frac{1}{3}\boldsymbol{C}\otimes\boldsymbol{C}^{-1}\otimes\boldsymbol{C}^{-1} - \mathbb{I}\tilde{\otimes}\boldsymbol{C}^{-1} + \boldsymbol{C}\otimes\mathbb{I}_{\boldsymbol{C}^{-1}} - \mathbb{I}\otimes\boldsymbol{C}^{-1}\right\}\,, \tag{35}$$

where we defined $\left\{\mathbb{I}\tilde{\otimes}\boldsymbol{C}^{-1}\right\}_{mnijkl} = \mathbb{I}_{mnkl}C^{-1}_{ij}$ in order to make the representation of $\mathbb{M}$ in closed format possible. The only tensor remaining undetermined in equation (34) is $\bar{\mathbb{C}}^{iso}$.

Its specific form depends on the underlying elastic potential Ψ^{iso}. As done for the isochoric part of the 2^{nd} PIOLA-KIRCHHOFF stresses, we will state a general representation of $\bar{\mathbb{C}}^{iso}$ for a free energy function of the form $\Psi^{iso} = \hat{\Psi}^{iso}(\bar{I}_1, \bar{I}_2)$. It reads

$$\bar{\mathbb{C}}^{iso} = 4\,\partial^2_{\bar{\boldsymbol{C}}\bar{\boldsymbol{C}}}\Psi^{iso}(\bar{I}_1, \bar{I}_2) = 4\,\partial_{\bar{\boldsymbol{C}}}(\partial_{\bar{I}_1}\Psi^{iso}\,\frac{\partial \bar{I}_1}{\partial \bar{\boldsymbol{C}}} + \partial_{\bar{I}_2}\Psi^{iso}\frac{\partial \bar{I}_2}{\partial \bar{\boldsymbol{C}}})\;. \tag{36}$$

Utilizing the free energy function of YEOH's model, after some steps we arrive at

$$\bar{\mathbb{C}}^{iso} = 8(C_{20} + 3C_{30}(\bar{I}_1 - 3))\boldsymbol{1} \otimes \boldsymbol{1}\;. \tag{37}$$

With all the tensors at hand, the isochoric part of the Lagrangian moduli $\mathbb{C}^{iso}$ can be calculated. In order to complete the additive representation of the total Lagrangian moduli $\mathbb{C}$, only the volumetric part $\mathbb{C}^{vol}$ remains to be determined. The expression needed for the derivation is obtained directly from equation (32), i.e.

$$\boxed{\mathbb{C}^{vol} = J(\Psi^{vol'} + J\Psi^{vol''})\boldsymbol{C}^{-1} \otimes \boldsymbol{C}^{-1} - 2J\Psi^{vol'}\mathbb{I}_{\boldsymbol{C}^{-1}}} \tag{38}$$

Up to now, we have derived a three-dimensional representation of YEOH's model for isotropic hyperelasticity at finite deformations.

3. Isotropic Finite Linear Viscoelasticity

In the previous section, we derived a finite hyperelasticity model, which is capable of describing the material behaviour of isotropic elastic rubber-like materials. This model will be extended to finite linear viscoelasticity within the forthcoming section. For more comprehensive literature concerning the subject of linear viscoelasticity, also refer to the standard textbooks written by SIMO & HUGHES [16], MALVERN [7] and CHRISTENSEN [3], or to the works of SIMO [14], GOVINDJEE [4] and KALISKE & ROTHERT [6] among many others.

3.1. Three-Dimensional Linear Viscoelasticity at Finite Strains

The next step in modeling viscoelastic materials is enabling a description valid for finite deformations. There are various approaches to the description of linear viscoelastic material behaviour at finite strains. The approach here is to consider the overall viscoelastic response with the volumetric-isochoric split, which is outlined in what follows.

3.1.1. Finite Linear Viscoelasticity with Volumetric-Isochoric Split

At this point, we assume that the viscous effects only have an isochoric contribution. Therefore, the volumetric deformations are considered as purely elastic. To this end, we use a free energy function having the general form

$$\begin{aligned}\Psi(\boldsymbol{C}, \boldsymbol{A}_1, \boldsymbol{A}_2, ..., \boldsymbol{A}_{n_v}) &= \Psi_{vol}(J) + \Psi_{iso}(\bar{\boldsymbol{C}}, \boldsymbol{A}_i)\\ &= \Psi_{vol}(J) + \Psi^e(\bar{\boldsymbol{C}}) + \sum_{i=1}^{n_v}\Psi^v_i(\bar{\boldsymbol{C}}, \boldsymbol{A}_i)\;,\end{aligned}$$

© 2007 Copyright by DYNAmore GmbH

where the elastic and viscous part remain seperated. For the finite deformation case, the additive split of the 2^{nd} PIOLA-KIRCHHOFF stresses reads

$$\boldsymbol{S} = \boldsymbol{S}_{vol} + \boldsymbol{S}_{iso} \, , \tag{39}$$

where

$$\begin{aligned} \boldsymbol{S}_{vol} &= J\Psi'_{vol}(J)\,\boldsymbol{C}^{-1} \\ \boldsymbol{S}_{iso} &= J^{-\frac{2}{3}}\,\mathrm{DEV}\left[\bar{\boldsymbol{S}}^e_{iso} + \sum_{i=1}^{n_v} \bar{\boldsymbol{Q}}_i\right] \\ &= \boldsymbol{S}^e_{iso} + \sum_{i=1}^{n_v} \boldsymbol{Q}_i \end{aligned} \tag{40}$$

with

$$\begin{aligned} \bar{\boldsymbol{S}}^e_{iso} &= 2\,\partial_{\bar{\boldsymbol{C}}}\Psi^e(\bar{\boldsymbol{C}}) \\ \bar{\boldsymbol{Q}}_i &= 2\,\partial_{\bar{\boldsymbol{C}}}\Psi^v_i(\bar{\boldsymbol{C}}, \boldsymbol{A}_i) \\ \mathrm{DEV}\,[\bullet] &= [\bullet] : \left[\mathbb{I} - \frac{1}{3}\boldsymbol{C} \otimes \boldsymbol{C}^{-1}\right] \, . \end{aligned} \tag{41}$$

For the computation of the isochoric viscous overstresses $\bar{\boldsymbol{Q}}_i$ we make use of the evolution equation

$$\boxed{\dot{\bar{\boldsymbol{Q}}}_i + \frac{1}{\tau_i}\bar{\boldsymbol{Q}}_i = \beta_i \frac{d}{dt}\left(\mathrm{DEV}\left[\bar{\boldsymbol{S}}^e_{iso}\right]\right)} \tag{42}$$

proposed by SIMO [14]. Note that integration of this evolution equation using the midpoint rule yields symmetric consistent Lagrangian moduli. The differential equation (42) can be solved by using the convolution form. Hence, we have to consider the identity

$$\frac{d}{dt}\left[\exp\left\{\frac{t}{\tau_i}\right\}\bar{\boldsymbol{Q}}_i\right] = \exp\left\{\frac{t}{\tau_i}\right\}\beta_i \frac{d}{dt}\left(\mathrm{DEV}\left[\bar{\boldsymbol{S}}^e_{iso}\right]\right) \, . \tag{43}$$

Following the integration from 0 to t, using the fundamental theorem of calculus and employing the initial condition $\bar{\boldsymbol{Q}}_i(t=0) = \boldsymbol{0}$, we get the representation for the viscous stresses as a function of time, i.e.

$$\boxed{\bar{\boldsymbol{Q}}_i(t) = \underbrace{\exp\left\{-\frac{t}{\tau_i}\right\}\bar{\boldsymbol{Q}}_i(0)}_{=0} + \int_0^t \exp\left\{-\frac{(t-s)}{\tau_i}\right\}\beta_i \frac{d}{ds}\left(\mathrm{DEV}\left[\bar{\boldsymbol{S}}^e_{iso}\right]\right) ds} \tag{44}$$

Following the well known steps, the equation above is solved using the convolution integral.

3.1.2. Algorithmic Setting for the Finite Strain Implementation

The convolution integral appearing in (44) must be treated numerically in order to come to a solution. To this end, we consider a time discretization with $\Delta t = t_{n+1} - t_n$. When doing so, $\bar{\boldsymbol{Q}}_i^{n+1}$ can be written as

$$\begin{aligned}\bar{\boldsymbol{Q}}_i^{n+1} &= \exp\left\{-\frac{\Delta t}{\tau_i}\right\} \underbrace{\int_0^{t_n} \exp\left\{-\frac{(t_n - s)}{\tau_i}\right\} \beta_i \frac{d}{ds}\left(\text{DEV}\left[\bar{\boldsymbol{S}}^e_{iso}\right]\right) ds}_{=\bar{\boldsymbol{Q}}_i^n} \\ &+ \int_{t_n}^{t_{n+1}} \exp\left\{-\frac{(t_{n+1} - s)}{\tau_i}\right\} \beta_i \frac{d}{ds}\left(\text{DEV}\left[\bar{\boldsymbol{S}}^e_{iso}\right]\right) ds \\ &= \exp\left\{-\frac{\Delta t}{\tau_i}\right\} \bar{\boldsymbol{Q}}_i^n + \int_{t_n}^{t_{n+1}} \exp\left\{-\frac{(t_{n+1} - s)}{\tau_i}\right\} \beta_i \frac{d}{ds}\left(\text{DEV}\left[\bar{\boldsymbol{S}}^e_{iso}\right]\right) ds\,. \quad (45)\end{aligned}$$

The second term on the right hand side of equation (45) may be integrated by making use of the mid-point rule, which is second-order accurate and unconditionally stable. Also setting

$$\frac{d}{ds}\left(\text{DEV}\left[\bar{\boldsymbol{S}}^e_{iso}\right]\right) = \frac{\left(\text{DEV}\left[\bar{\boldsymbol{S}}^{e,n+1}_{iso}\right] - \text{DEV}\left[\bar{\boldsymbol{S}}^{e,n}_{iso}\right]\right)}{\Delta t}\,,$$

in equation (45) and collecting the terms belonging to time t_n, we obtain the update equation for the viscous stresses at time t_{n+1} according to

$$\begin{aligned}\bar{\boldsymbol{Q}}_i^{n+1} &= \bar{\boldsymbol{H}}_i^n + \exp\left\{-\frac{\Delta t}{2\tau_i}\right\} \beta_i\, J_{n+1}^{\frac{2}{3}} \boldsymbol{S}^{e,n+1}_{iso} \\ \text{with} \quad \bar{\boldsymbol{H}}_i^{n+1} &= \exp\left\{-\frac{\Delta t}{\tau_i}\right\} \bar{\boldsymbol{Q}}_i^{n+1} - \exp\left\{-\frac{\Delta t}{2\tau_i}\right\} \beta_i\, J_{n+1}^{\frac{2}{3}} \boldsymbol{S}^{e,n+1}_{iso}\,. \quad (46)\end{aligned}$$

In this representation $\bar{\boldsymbol{H}}_i^n$ are the history variables to be stored in a finite element implementation. The total 2^{nd} PIOLA-KIRCHHOFF stresses at time t_{n+1} then follow according to

$$\boldsymbol{S}^{n+1} = \boldsymbol{S}^{n+1}_{vol} + \boldsymbol{S}^{n+1}_{iso}\,.$$

The specific form of the isochoric 2^{nd} PIOLA-KIRCHHOFF stresses will be derived in the following.

$$\begin{aligned}\boldsymbol{S}^{n+1}_{iso} &= J_{n+1}^{-\frac{2}{3}}\, \text{DEV}\left[\bar{\boldsymbol{S}}^{e,n+1}_{iso} + \sum_{i=1}^{n_v} \bar{\boldsymbol{Q}}_i^{n+1}\right] \\ &\overset{(46)}{=} \boldsymbol{S}^{e,n+1}_{iso} + J_{n+1}^{-\frac{2}{3}}\, \text{DEV}\left[\sum_{i=1}^{n_v}\left(\bar{\boldsymbol{H}}_i^n + \exp\left\{-\frac{\Delta t}{2\tau_i}\right\} \beta_i\, J_{n+1}^{\frac{2}{3}} \boldsymbol{S}^{e,n+1}_{iso}\right)\right] \\ &= \boldsymbol{S}^{e,n+1}_{iso} + \sum_{i=1}^{n_v} \beta_i \exp\left\{-\frac{\Delta t}{2\tau_i}\right\} \boldsymbol{S}^{e,n+1}_{iso} + \sum_{i=1}^{n_v} J_{n+1}^{-\frac{2}{3}}\, \text{DEV}\left[\bar{\boldsymbol{H}}_i^n\right]\,, \quad (47)\end{aligned}$$

where we made use of the identity

$$\text{DEV}\left[\text{DEV}\left[\bullet\right]\right] = \text{DEV}\left[\bullet\right]\,, \quad (48)$$

 © 2007 Copyright by DYNAmore GmbH

leading to

$$\mathrm{DEV}\left[\boldsymbol{S}^{e,n+1}_{iso}\right] = \boldsymbol{S}^{e,n+1}_{iso} = J^{-\frac{2}{3}}_{n+1}\,\mathrm{DEV}\left[\bar{\boldsymbol{S}}^{e,n+1}_{iso}\right] \; . \tag{49}$$

Also defining

$$\boldsymbol{H}^{n}_{i} = \bar{\boldsymbol{H}}^{n}_{i} : \mathbb{Q}_{n+1} = J^{-\frac{2}{3}}_{n+1}\,\mathrm{DEV}\left[\bar{\boldsymbol{H}}^{n}_{i}\right] \; , \tag{50}$$

we finally arrive at the representation for the isochoric 2^{nd} PIOLA-KIRCHHOFF stresses

$$\boldsymbol{S}^{n+1}_{iso} = \underbrace{\left[1 + \sum_{i=1}^{n_v} \beta_i \exp\left\{-\frac{\Delta t}{2\tau_i}\right\}\right]}_{=:\,g(\Delta t)} \boldsymbol{S}^{e,n+1}_{iso} + \sum_{i=1}^{n_v} \bar{\boldsymbol{H}}^{n}_{i} : \mathbb{Q}_{n+1} \tag{51}$$

The volumetric part of the 2^{nd} PIOLA-KIRCHHOFF stresses at time t_{n+1} are obtained from (40), i.e.

$$\boldsymbol{S}^{n+1}_{vol} = J_{n+1}\Psi'_{vol}(J_{n+1})\,\boldsymbol{C}^{-1}_{n+1} \; . \tag{52}$$

To finalize the formulation, we once more have to derive the equations for the symmetric consistent Lagrangian moduli

$$\mathbb{C} = \mathbb{C}_{vol} + \mathbb{C}_{iso} \; , \tag{53}$$

where the specific form of the volumetric part is

$$\mathbb{C}_{vol} = 2\,\partial_{\boldsymbol{C}}\boldsymbol{S}_{vol} = \left(J^2\,\Psi''_{vol}(J) + J\,\Psi'_{vol}(J)\right)\boldsymbol{C}^{-1}\otimes\boldsymbol{C}^{-1} - 2J\,\Psi'_{vol}(J)\,\mathbb{I}_{\boldsymbol{C}^{-1}} \tag{54}$$

and the isochoric part is given by the expression

$$\begin{aligned} \mathbb{C}^{n+1}_{iso} &= \partial_{\boldsymbol{C}_{n+1}}\left(\boldsymbol{S}^{n+1}_{iso}\right) \\ &= \underbrace{\left[1 + \sum_{i=1}^{n_v} \beta_i \exp\left\{-\frac{\Delta t}{2\tau_i}\right\}\right]}_{=:\,g(\Delta t)} \mathbb{C}^{e,n+1}_{iso} + \sum_{i=1}^{n_v} \bar{\boldsymbol{H}}^{n}_{i} : \mathbb{M}_{n+1} \; , \end{aligned} \tag{55}$$

where

$$\begin{aligned} \mathbb{C}^{e,n+1}_{iso} &= \mathbb{Q}^{T}_{n+1} : \bar{\mathbb{C}}^{e,n+1}_{iso} : \mathbb{Q}_{n+1} + \bar{\boldsymbol{S}}^{e,n+1}_{iso} : \mathbb{M}_{n+1} \\ \bar{\boldsymbol{S}}^{e,n+1}_{iso} &= 2\,\partial_{\bar{\boldsymbol{C}}}\Psi^{e}(\bar{\boldsymbol{C}}_{n+1}) \\ \bar{\mathbb{C}}^{e,n+1}_{iso} &= 4\,\partial^2_{\bar{\boldsymbol{C}}\bar{\boldsymbol{C}}}\Psi^{e}(\bar{\boldsymbol{C}}_{n+1}) = 2\,\partial_{\bar{\boldsymbol{C}}}\bar{\boldsymbol{S}}^{e,n+1}_{iso} \; . \end{aligned} \tag{56}$$

4. Anisotropic Finite Linear Viscoelasticity

Up to now we have derived the governing equations necessary for describing isotropic elastic and linear viscoelastic material behaviour. To make the introduction of the notion of anisotropy as comprehensive as possible, the basic terms and definitions are given, which then are applied to the finite deformation theory. Several aspects of the theory of invariants are discussed, which is inevitable for describing the anisotropic material response at finite deformations, because we account for the anisotropy using a coordinate free representation with structural tensors. In the last step, we postulate a concrete free energy function and derive the governing equations for an orthotropic finite linear viscoelasticity model, in which transverse isotropy is included as a special case.

For an in-depth discussion of the subject of anisotropy, also consider the literature provided by BOEHLER [2], TRUESDELL & NOLL [20], SPENCER [17, 18], APEL [1] ,RIEGER [11] and SCHRÖDER [12] among many others.

4.1. Definition of an Anisotropic Material

As already outlined in Section 3.1, a material is called anisotropic, if an arbitrary transformation $\boldsymbol{Q}$ applied to the material's internal structure does not map the structure onto itself and therefore leads to a different stress response. Since we consider a coordinate free representation of anisotropy in terms of isotropic tensor functions using structural tensors, the function Ψ with the extended set of arguments is an isotropic tensor function, if

$$\hat{\Psi}(\boldsymbol{QCQ}^T, \boldsymbol{QMQ}^T) = \hat{\Psi}(\boldsymbol{C}, \boldsymbol{M}) \qquad \forall\, \boldsymbol{Q} \in \mathcal{SO}(3) \tag{57}$$

holds, where $\boldsymbol{M}$ is the constant second-order structural tensor characterizing the directional dependence of the particular anisotropic response. Again, $\boldsymbol{M}$ must be defined such that

$$\hat{\Psi}(\boldsymbol{QCQ}^T, \boldsymbol{M}) = \hat{\Psi}(\boldsymbol{C}, \boldsymbol{M}) \qquad \forall\, \boldsymbol{Q} \in \mathcal{G} \subset \mathcal{SO}(3)\,. \tag{58}$$

When trying to express the free energy function Ψ as an isotropic tensor function with several arguments, we need to establish a so-called integrity basis, which defines a minimum number of invariants for a particular set of argument tensors. Tables of such integrity bases may be found in SPENCER [17, 18] and BOEHLER [2].

For a symmetric second-order tensor $\boldsymbol{A}$ the minimal integrity basis reads

$$\mathrm{tr}[\boldsymbol{A}], \quad \mathrm{tr}\left[\boldsymbol{A}^2\right], \quad \mathrm{tr}\left[\boldsymbol{A}^3\right], \tag{59}$$

which are the basic invariants $\{J_i\}_{i=1,2,3}$ of the tensor $\boldsymbol{A}$. Note that it is also possible to state the minimal integrity basis in terms of the principal invariants $\{I_i\}_{i=1,2,3}$. They are linked to the basic invariants according to

$$\begin{aligned} J_1 &= I_1 \\ J_2 &= I_1^2 - 2I_2 \\ J_3 &= I_1^3 - 3I_1I_2 + 3I_3\,. \end{aligned} \tag{60}$$

When considering two symmetric second-order tensors $\boldsymbol{A}$ and $\boldsymbol{B}$, the minimal integrity basis is given by

$$\begin{gathered} \mathrm{tr}[\boldsymbol{A}], \quad \mathrm{tr}\left[\boldsymbol{A}^2\right], \quad \mathrm{tr}\left[\boldsymbol{A}^3\right], \quad \mathrm{tr}[\boldsymbol{B}], \quad \mathrm{tr}\left[\boldsymbol{B}^2\right], \quad \mathrm{tr}\left[\boldsymbol{B}^3\right], \\ \mathrm{tr}[\boldsymbol{AB}], \quad \mathrm{tr}\left[\boldsymbol{AB}^2\right], \quad \mathrm{tr}\left[\boldsymbol{A}^2\boldsymbol{B}\right], \quad \mathrm{tr}\left[\boldsymbol{A}^2\boldsymbol{B}^2\right]\,. \end{gathered} \tag{61}$$

It consists of the basic invariants of the two argument tensors and the so-called mixed invariants composed of the two. In the case of three symmetric second-order tensors $\boldsymbol{A}$,

© 2007 Copyright by DYNAmore GmbH

$\boldsymbol{B}$ and $\boldsymbol{C}$, the minimal integrity basis comprises the correspondent invariants stated in equations (59) and (61) and the additional terms

$$\begin{aligned}\mathrm{tr}[\boldsymbol{ABC}],\quad \mathrm{tr}\left[\boldsymbol{A}^2\boldsymbol{BC}\right],\quad \mathrm{tr}\left[\boldsymbol{B}^2\boldsymbol{CA}\right],\ \mathrm{tr}\left[\boldsymbol{C}^2\boldsymbol{AB}\right],\\ \mathrm{tr}\left[\boldsymbol{A}^2\boldsymbol{B}^2\boldsymbol{C}\right],\quad \mathrm{tr}\left[\boldsymbol{B}^2\boldsymbol{C}^2\boldsymbol{A}\right],\quad \mathrm{tr}\left[\boldsymbol{C}^2\boldsymbol{A}^2\boldsymbol{B}\right]\ .\end{aligned} \tag{62}$$

Since we will deal with an orthotropic material in the following, the minimal integrity basis of three symmetric second-order tensors is sufficient.

4.2. Minimal Integrity Basis for an Orthotropic Material

An orthotropic material has three preferred directions. These three directions $\boldsymbol{a}_1$, $\boldsymbol{a}_2$ and $\boldsymbol{a}_3$ compose an orthonormal basis. The symmetry group of an orthotropic material is characterized by

$$\mathcal{G} = \{\boldsymbol{1}, -\boldsymbol{1}, \boldsymbol{Q}^{\pi}_{\perp\boldsymbol{a}_1}, \boldsymbol{Q}^{\pi}_{\perp\boldsymbol{a}_2}, \boldsymbol{Q}^{\pi}_{\perp\boldsymbol{a}_3}, \boldsymbol{D}_1, \boldsymbol{D}_2, \boldsymbol{D}_3\}\ , \tag{63}$$

Here, $\boldsymbol{Q}^{\pi}_{\perp\boldsymbol{a}_1}$,$\boldsymbol{Q}^{\pi}_{\perp\boldsymbol{a}_2}$ and $\boldsymbol{Q}^{\pi}_{\perp\boldsymbol{a}_3}$ are reflections with respect to the planes $(\boldsymbol{a}_2, \boldsymbol{a}_3)$, $(\boldsymbol{a}_3, \boldsymbol{a}_1)$ and $(\boldsymbol{a}_1, \boldsymbol{a}_2)$, which are perpendicular to the three anisotropy directions. The composition of two reflections is denoted as $\{\boldsymbol{D}_i\}_{i=1,2,3}$, i.e. $\boldsymbol{D}_1 = \boldsymbol{Q}^{\pi}_{\perp\boldsymbol{a}_2}\boldsymbol{Q}^{\pi}_{\perp\boldsymbol{a}_3}$. One can think of an orthotropic material as a material composed of two different fibers, which lie perpendicular to each other. The third anisotropy direction is defined by the cross product of these two fiber directions. The second-order structural tensors are calculated with the dyadic product of the preferred directions $\{\boldsymbol{a}_i\}_{i=1,2,3}$ with themselves, i.e.

$$\boldsymbol{M}_i := \boldsymbol{a}_i \otimes \boldsymbol{a}_i \quad \forall\ i = 1, 2, 3\ . \tag{64}$$

As mentioned above, the structural tensors have to be invariant under rotations $\boldsymbol{Q}$ out of the symmetry group $\mathcal{G}$, which means that they have to satisfy the condition

$$\boldsymbol{M}_i = \boldsymbol{Q}\boldsymbol{M}_i\boldsymbol{Q}^T \quad \forall\ \boldsymbol{Q} \in \mathcal{G}\ . \tag{65}$$

Therefore, the free energy function Ψ to be established consequently is an isotropic tensor function in terms of the argument tensors $\bar{\boldsymbol{C}}, \boldsymbol{M}_1, \boldsymbol{M}_2$ and $\boldsymbol{M}_3$. Due to the fact that the three vectors $\boldsymbol{a}_1, \boldsymbol{a}_2$ and $\boldsymbol{a}_3$ are orthonormal and $\boldsymbol{a}_3 = \boldsymbol{a}_1 \times \boldsymbol{a}_2$ holds, the third anisotropy direction may be expressed in terms of the other two. Hence, the second-order tensor $\boldsymbol{M}_3$ of the third direction is linearly dependent on $\boldsymbol{M}_1$ and $\boldsymbol{M}_2$. The condition arising from this reads

$$\boldsymbol{M}_3 = \boldsymbol{1} - \boldsymbol{M}_1 - \boldsymbol{M}_2 \tag{66}$$

and therefore the free energy function Ψ of an othotropic material is only dependent on the isochoric part of the right Cauchy-Green tensor $\bar{\boldsymbol{C}}$ and on the two structural tensors $\boldsymbol{M}_1$ and $\boldsymbol{M}_2$, i.e.

$$\Psi = \hat{\Psi}(\bar{\boldsymbol{C}}, \boldsymbol{M}_1, \boldsymbol{M}_2)\ . \tag{67}$$

Since an important feature of the structural tensors is their orthogonality, the scalar product of two of these second-order tensors must equal zero

$$\boldsymbol{M}_1 : \boldsymbol{M}_2 = (\boldsymbol{a}_1 \otimes \boldsymbol{a}_1) : (\boldsymbol{a}_2 \otimes \boldsymbol{a}_2) = 0\ . \tag{68}$$

As a result of this orthogonality condition, the mixed invariants stated in equation (62) may be omitted when defining the minimal integrity basis. In addition to this, one has to consider that the first-order anisotropy tensors $\{\boldsymbol{a}_i\}_{i=1,2,3}$ are of unit length, this is $\|\boldsymbol{a}_i\| = 1$ for $i = 1, 2, 3$. From this follows that every power of a structural tensor is the structural tensor itself

$$\boldsymbol{M}_i^2 = \boldsymbol{M}_i \quad \forall\ i = 1, 2, 3\,. \tag{69}$$

Taking equations (66) and (69) into account, the integrity basis of an orthotropic material composed of the basic and mixed invariants of the isochoric right CAUCHY-GREEN tensor and the two structural tensors $\boldsymbol{M} = \boldsymbol{a}_1 \otimes \boldsymbol{a}_1$ and $\boldsymbol{N} = \boldsymbol{a}_2 \otimes \boldsymbol{a}_2$ is given by

$$\boldsymbol{\mathcal{I}} = \{\bar{J}_1, \bar{J}_2, \bar{J}_3, \bar{J}_4, \bar{J}_5, \bar{J}_6, \bar{J}_7, \bar{I}_{\boldsymbol{M}}, \bar{I}_{\boldsymbol{M}}\}\,, \tag{70}$$

or with the definitions of the invariants

$$\begin{aligned}\boldsymbol{\mathcal{I}} \;=\; & \Big\{\mathrm{tr}\big[\bar{\boldsymbol{C}}\big], \mathrm{tr}\Big[\bar{\boldsymbol{C}}^2\Big], \mathrm{tr}\Big[\bar{\boldsymbol{C}}^3\Big], \mathrm{tr}\big[\bar{\boldsymbol{C}}\boldsymbol{M}\big], \mathrm{tr}\Big[\bar{\boldsymbol{C}}^2\boldsymbol{M}\Big], \\ & \mathrm{tr}\big[\bar{\boldsymbol{C}}\boldsymbol{N}\big], \mathrm{tr}\Big[\bar{\boldsymbol{C}}^2\boldsymbol{N}\Big], \mathrm{tr}[\boldsymbol{M}], \mathrm{tr}[\boldsymbol{N}]\Big\}\;.\end{aligned} \tag{71}$$

Note that the traces of the structural tensors are constant, i.e. $\mathrm{tr}[\boldsymbol{M}] = 1$ and $\mathrm{tr}[\boldsymbol{N}] = 1$. An alternative representation of equations (70) and (71) would be a mixture of the principal invariants $\{I_i\}_{i=1,2,3}$ and the mixed invariants $\{J_j\}_{j=4,5,6,7}$

$$\boldsymbol{\mathcal{I}} = \{\bar{I}_1, \bar{I}_2, \bar{I}_3, \bar{J}_4, \bar{J}_5, \bar{J}_6, \bar{J}_7, \bar{I}_{\boldsymbol{M}}, \bar{I}_{\boldsymbol{M}}\}\,, \tag{72}$$

which leads to

$$\begin{aligned}\boldsymbol{\mathcal{I}} \;=\; & \Big\{\mathrm{tr}\big[\bar{\boldsymbol{C}}\big], \mathrm{tr}\big[\mathrm{cof}\,\bar{\boldsymbol{C}}\big],\ \det\big[\bar{\boldsymbol{C}}\big], \mathrm{tr}\big[\bar{\boldsymbol{C}}\boldsymbol{M}\big], \mathrm{tr}\Big[\bar{\boldsymbol{C}}^2\boldsymbol{M}\Big], \\ & \mathrm{tr}\big[\bar{\boldsymbol{C}}\boldsymbol{N}\big], \mathrm{tr}\Big[\bar{\boldsymbol{C}}^2\boldsymbol{N}\Big], \mathrm{tr}[\boldsymbol{M}], \mathrm{tr}[\boldsymbol{N}]\Big\}\;.\end{aligned} \tag{73}$$

Since $\bar{I}_3 = \det\big[\bar{\boldsymbol{C}}\big] = 1$, this invariant has not to be included in the free energy function. Equations (70) and (72) state the minimal integrity basis necessary for describing the free energy function of an orthotropic material by means of an isotropic tensor function.

4.3. Orthotropic Elasticity

In the previous section, we have provided the framework for the definition of a free energy function Ψ accounting for orthotropic material behaviour. In this section we establish a concrete form of such a free energy function for an orthotropic elastic material and we derive the constitutive equations for the 2^{nd} PIOLA-KIRCHHOFF stresses and the Lagrangian moduli.

We stick to the premise that the free energy function is split additively into volumetric and isochoric parts. Additionally, we split the isochoric part into an isotropic and an anisotropic part according to

$$\Psi(\bar{\boldsymbol{C}}, \boldsymbol{M}, \boldsymbol{N}) = \Psi_I(\bar{\boldsymbol{C}}) + \Psi_A(\bar{\boldsymbol{C}}, \boldsymbol{M}, \boldsymbol{N})\,, \tag{74}$$

© 2007 Copyright by DYNA*more* GmbH

where the subscripts I and A stand for isotropic and anisotropic, respectively. The superscript iso is dropped in the equation above, since only the isochoric part of the free energy function Ψ is considered in the following. For the definition of the free energy function, we make use of the integrity basis stated in equation (72). The isotropic elastic part is characterized by the free energy function of YEOH's model

$$\Psi_I = C_{10}(\bar{I}_1 - 3) + C_{20}(\bar{I}_1 - 3)^2 + C_{30}(\bar{I}_1 - 3)^3$$

and the anisotropic part will be represented by the isotropic polynomial tensor function

$$\Psi_A = \alpha_{e1}(\bar{J}_4 - 1)^2 + \alpha_{e2}K_{11} + \alpha_{e3}(\bar{J}_6 - 1)^2 + \alpha_{e4}K_{12} \ , \tag{75}$$

where K_{11} and K_{12} are polyconvex polynomials in terms of non-polyconvex invariants $\bar{J}_5$, $\bar{J}_4\bar{I}_1$, $\bar{J}_7$ and $\bar{J}_6\bar{I}_1$. According to SCHRÖDER & NEFF [13], they are defined as follows

$$\begin{aligned} K_{11} &= (\bar{J}_5 - 1) - (\bar{I}_1 - 3)(\bar{J}_4 - 1) + (\bar{I}_2 - 3) \\ K_{12} &= (\bar{J}_7 - 1) - (\bar{I}_1 - 3)(\bar{J}_6 - 1) + (\bar{I}_2 - 3) \ . \end{aligned} \tag{76}$$

Note that K_{11} holds for the preferred direction $\boldsymbol{a}_1$ and K_{12} accounts for the preferred direction $\boldsymbol{a}_2$. Hence, the preferred directions $\boldsymbol{a}_1$ and $\boldsymbol{a}_2$ are decoupled in equation (75). Therefore, the model may also be used in order to describe transverse isotropy when setting either $\alpha_{e1} = \alpha_{e2} = 0$ or $\alpha_{e3} = \alpha_{e4} = 0$, respectively. The entire free energy function unavoidably needs to be extended according to

$$\Psi = \Psi_I + \Psi_A + \Psi_{\boldsymbol{M}} + \Psi_{\boldsymbol{N}} \ , \tag{77}$$

where $\Psi_{\boldsymbol{M}}$ and $\Psi_{\boldsymbol{N}}$ are functions which are introduced in order to fulfill the condition of a stress free reference configuration with respect to the so-called tensor generators $\boldsymbol{M}$ and $\boldsymbol{N}$. In our case they are identified as

$$\begin{aligned} \Psi_{\boldsymbol{M}} &= -2\alpha_{e2}(\bar{J}_4 - 1) \\ \Psi_{\boldsymbol{N}} &= -2\alpha_{e4}(\bar{J}_6 - 1) \ . \end{aligned}$$

Since we now have defined the free energy function for the orthotropic elasticity model, we need to derive the 2^{nd} PIOLA-KIRCHHOFF stresses and the Lagrangian moduli.

2^{nd} Piola-Kirchhoff Stresses

As already done in equation (20), the isochoric part of the 2^{nd} PIOLA-KIRCHHOFF stresses is derived from the free energy function according to

$$\boldsymbol{S}^{iso} = 2\partial_{\boldsymbol{C}}\Psi^{iso} = 2\partial_{\bar{\boldsymbol{C}}}\Psi^{iso} : \partial_{\boldsymbol{C}}\bar{\boldsymbol{C}} = \bar{\boldsymbol{S}}^{iso} : \mathbb{Q} \ .$$

Since Ψ is expressed in terms of the invariants, we obtain the following equation for the isochoric chain rule stresses

$$\boxed{\bar{\boldsymbol{S}}^{iso} = 2 \sum_{L_i \in \boldsymbol{\mathcal{I}} \setminus \bar{I}_{\boldsymbol{M}}, \bar{I}_{\boldsymbol{N}}} \frac{\partial \Psi}{\partial L_i} \frac{\partial L_i}{\partial \bar{\boldsymbol{C}}}} \tag{78}$$

The tensor generators $\partial_{\bar{C}} L_i$ are given by

$$\begin{aligned}
\partial_{\bar{\boldsymbol{C}}} L_1 := \partial_{\bar{\boldsymbol{C}}} \bar{I}_1 &= \boldsymbol{1} \\
\partial_{\bar{\boldsymbol{C}}} L_2 := \partial_{\bar{\boldsymbol{C}}} \bar{I}_2 &= (\bar{I}_1 \boldsymbol{1} - \bar{\boldsymbol{C}}) \\
\partial_{\bar{\boldsymbol{C}}} L_4 := \partial_{\bar{\boldsymbol{C}}} \bar{J}_4 &= \boldsymbol{M} \\
\partial_{\bar{\boldsymbol{C}}} L_5 := \partial_{\bar{\boldsymbol{C}}} \bar{J}_5 &= (\boldsymbol{M}\bar{\boldsymbol{C}} + \bar{\boldsymbol{C}}\boldsymbol{M}) \\
\partial_{\bar{\boldsymbol{C}}} L_6 := \partial_{\bar{\boldsymbol{C}}} \bar{J}_6 &= \boldsymbol{N} \\
\partial_{\bar{\boldsymbol{C}}} L_7 := \partial_{\bar{\boldsymbol{C}}} \bar{J}_7 &= (\boldsymbol{N}\bar{\boldsymbol{C}} + \bar{\boldsymbol{C}}\boldsymbol{N})
\end{aligned} \tag{79}$$

and the derivatives of the free energy function with respect to the invariants $\partial_{L_i}\Psi$ read

$$\begin{aligned}
\partial_{\bar{I}_1}\Psi &= \left[C_{10} + 2C_{20}(\bar{I}_3 - 3) + 3C_{30}(\bar{I}_3 - 3)^2 - (\alpha_{e2}(\bar{J}_4 - 1) + \alpha_{e4}(\bar{J}_6 - 1))\right] \\
\partial_{\bar{I}_2}\Psi &= (\alpha_{e3} + \alpha_{e4}) \\
\partial_{\bar{J}_4}\Psi &= \left[2\alpha_{e1}(\bar{J}_4 - 1) - 2\alpha_{e2}\right] \\
\partial_{\bar{J}_5}\Psi &= \alpha_{e2} \\
\partial_{\bar{J}_6}\Psi &= \left[2\alpha_{e3}(\bar{J}_6 - 1) - 2\alpha_{e4}\right] \\
\partial_{\bar{I}_7}\Psi &= \alpha_{e4}
\end{aligned} \tag{80}$$

Application of equation (78) to (77) and making use of equations (79) and (80) yields

$$\bar{\boldsymbol{S}}^{iso} = f_1\,\boldsymbol{1} + f_2\,\bar{\boldsymbol{C}} + f_3\,\boldsymbol{M} + f_4\,(\boldsymbol{M}\bar{\boldsymbol{C}} + \bar{\boldsymbol{C}}\boldsymbol{M}) + f_5\,\boldsymbol{N} + f_6\,(\boldsymbol{N}\bar{\boldsymbol{C}} + \bar{\boldsymbol{C}}\boldsymbol{N})\,, \tag{81}$$

with the scalar valued functions $\{f_i\}_{i=1,\dots,6}$, which are polynomials in terms of the invariants of the integrity basis $\boldsymbol{\mathcal{I}}$. For the specific free energy function defined above, they have the form

$$\begin{aligned}
f_1 &:= 2C_{10} + 4C_{20}(\bar{I}_3 - 3) + 6C_{30}(\bar{I}_3 - 3)^2 \\
&\quad + 2(\alpha_{e2} + \alpha_{e4})\bar{I}_1 - 2(\alpha_{e2}(\bar{J}_4 - 1) + \alpha_{e4}(\bar{J}_4 - 1)) \\
f_2 &:= -2(\alpha_{e2} + \alpha_{e4}) = \text{const.} \\
f_3 &:= 4\alpha_{e1}(\bar{J}_4 - 1) - 2\alpha_{e2}(\bar{I}_1 - 3) - 4\alpha_{e2} \\
f_4 &:= 2\alpha_{e2} = \text{const.} \\
f_5 &:= 4\alpha_{e3}(\bar{J}_6 - 1) - 2\alpha_{e4}(\bar{I}_1 - 3) - 4\alpha_{e4} \\
f_6 &:= 2\alpha_{e4} = \text{const.}
\end{aligned} \tag{82}$$

Lagrangian Moduli

The isochoric part defined in equation (34) reads

$$\mathbb{C}^{iso} = \mathbb{Q}^T : \bar{\mathbb{C}}^{iso} : \mathbb{Q} + \bar{\boldsymbol{S}}^{iso} : \mathbb{M}$$

and for the isochoric chain rule moduli $\bar{\mathbb{C}}^{iso}$ we obtain the following general form

© 2007 Copyright by DYNA*more* GmbH

$$\bar{\mathbb{C}}^{iso} = 4 \sum_{L_i \in \boldsymbol{\mathcal{I}} \setminus \bar{I}_{\boldsymbol{M}}, \bar{I}_{\boldsymbol{N}}} \left[\sum_{L_j \in \boldsymbol{\mathcal{I}} \setminus \bar{I}_{\boldsymbol{M}}, \bar{I}_{\boldsymbol{N}}} \left[\frac{\partial^2 \Psi}{\partial L_i \partial L_j} \frac{L_i}{\bar{\boldsymbol{C}}} \otimes \frac{L_j}{\bar{\boldsymbol{C}}} + \frac{\partial \Psi}{\partial L_i} \frac{\partial^2 L_i}{\partial \bar{\boldsymbol{C}} \partial \bar{\boldsymbol{C}}} \right] \right] \tag{83}$$

For the non-zero second derivatives of the free energy function, we get

$$\begin{aligned}
\partial^2_{\bar{I}_1 \bar{I}_1} \Psi &= \left[2C_{20} + 6C_{30}(\bar{I}_3 - 3) \right] \\
\partial^2_{\bar{I}_1 \bar{J}_4} \Psi &= -\alpha_{e2} \\
\partial^2_{\bar{I}_1 \bar{J}_6} \Psi &= -\alpha_{e4} \\
\partial^2_{\bar{J}_4 \bar{I}_1} \Psi &= -\alpha_{e2} \\
\partial^2_{\bar{J}_4 \bar{J}_4} \Psi &= 2\alpha_{e1} \\
\partial^2_{\bar{J}_6 \bar{I}_1} \Psi &= -\alpha_{e4} \\
\partial^2_{\bar{J}_6 \bar{J}_6} \Psi &= 2\alpha_{e3}
\end{aligned}$$

In an analogous manner we obtain the non-zero second derivatives of the tensor generators defined in equation (79). We end up with

$$\begin{aligned}
\partial^2_{\bar{\boldsymbol{C}}\bar{\boldsymbol{C}}} \bar{I}_2 &= \boldsymbol{1} \otimes \boldsymbol{1} - \mathbb{I} \\
\partial^2_{\bar{\boldsymbol{C}}\bar{\boldsymbol{C}}} \bar{J}_5 &= (\boldsymbol{M} \tilde{\otimes} \boldsymbol{1} + \boldsymbol{1} \tilde{\otimes} \boldsymbol{M}) \\
\partial^2_{\bar{\boldsymbol{C}}\bar{\boldsymbol{C}}} \bar{J}_7 &= (\boldsymbol{N} \tilde{\otimes} \boldsymbol{1} + \boldsymbol{1} \tilde{\otimes} \boldsymbol{N}) \, ,
\end{aligned} \tag{84}$$

using the definition $\left\{ \boldsymbol{A} \tilde{\otimes} \boldsymbol{B} \right\}_{ijkl} := \frac{1}{2}(A_{ik}B_{jl} + B_{ik}A_{il})$. With these results at hand, the Lagrangian chain rule moduli read

$$\begin{aligned}
\bar{\mathbb{C}}^{iso} &= g_1 \, \boldsymbol{1} \otimes \boldsymbol{1} + g_2 \, (\boldsymbol{M} \otimes \boldsymbol{1} + \boldsymbol{1} \otimes \boldsymbol{M}) + g_3 \, \boldsymbol{M} \otimes \boldsymbol{M} + g_4 \, (\boldsymbol{M} \tilde{\otimes} \boldsymbol{1} + \boldsymbol{1} \tilde{\otimes} \boldsymbol{M}) \\
&+ g_5 \, \mathbb{I} + g_6 \, (\boldsymbol{N} \otimes \boldsymbol{1} + \boldsymbol{1} \otimes \boldsymbol{N}) + g_7 \, \boldsymbol{N} \otimes \boldsymbol{N} + g_8 \, (\boldsymbol{N} \tilde{\otimes} \boldsymbol{1} + \boldsymbol{1} \tilde{\otimes} \boldsymbol{N}) \, ,
\end{aligned} \tag{85}$$

with the scalar valued functions $\{g_i\}_{i=1,\dots,8}$, which are also polynomials in terms of the invariants of the integrity basis $\mathcal{I}$. They have the form

$$\begin{aligned}
g_1 &:= \left[8C_{20} + 24C_{30}(\bar{I}_3 - 3) + 4(\alpha_{e2} + \alpha_{e4}) \right] \\
g_2 &:= -4\alpha_{e2} = \text{const.} \\
g_3 &:= 8\alpha_{e1} = \text{const.} \\
g_4 &:= 4\alpha_{e3} = \text{const.} \\
g_5 &:= -4(\alpha_{e2} + \alpha_{e4}) = \text{const.} \\
g_6 &:= -4\alpha_{e4} = \text{const.} \\
g_7 &:= 8\alpha_{e3} = \text{const.} \\
g_8 &:= 4\alpha_{e4} = \text{const.}
\end{aligned} \tag{86}$$

The equation for $\bar{\mathbb{C}}^{iso}$ completes the formulation of the orthotropic elastic material model at finite deformations.

© 2007 Copyright by DYNA*more* GmbH

4.4. Orthotropic Finite Linear Viscoelasticity

The aim of this section is the definition of a Helmholtz free energy function for an orthotropic linear viscoelaticity model and the derivation of the constitutive equations, see also the recent work by HOLZAPFEL & GASSER [5].

The free energy function is stated in an analogous fashion to the isotropic linear viscoelasticity model in Section 3.1.1. To make a clearer distinction between the internal strain-like variables and the preferred directions $\boldsymbol{a}_1$,$\boldsymbol{a}_2$ and $\boldsymbol{a}_3$, the latter are denoted as $\boldsymbol{a}$, $\boldsymbol{b}$ and $\boldsymbol{c}$. We preserve the volumetric-isochoric split of the free energy function and in a further step we additionally split the isochoric part into an elastic and a viscous contribution according to

$$\Psi^{iso}(\bar{\boldsymbol{C}}, \boldsymbol{M}, \boldsymbol{N}, \boldsymbol{\mathcal{I}}_i, \boldsymbol{\mathcal{A}}_j, \boldsymbol{\mathcal{B}}_k) = \Psi^e(\bar{\boldsymbol{C}}, \boldsymbol{M}, \boldsymbol{N}) + \Psi^v(\bar{\boldsymbol{C}}, \boldsymbol{M}, \boldsymbol{N}, \boldsymbol{\mathcal{I}}_i, \boldsymbol{\mathcal{A}}_j, \boldsymbol{\mathcal{B}}_k) \tag{87}$$

where $\boldsymbol{M} := \boldsymbol{a} \otimes \boldsymbol{a}$ and $\boldsymbol{N} := \boldsymbol{b} \otimes \boldsymbol{b}$ are the structural tensors for the corresponding preferred direction, $\boldsymbol{\mathcal{I}}_i$ are the strain-like internal variables for the isotropic linear viscoelastic part and $\boldsymbol{\mathcal{A}}_j$ as well as $\boldsymbol{\mathcal{B}}_k$ stand for the strain-like internal variables corresponding to the directions $\boldsymbol{a}$ and $\boldsymbol{b}$, respectively. Also we split both the elastic and viscous part of the free energy function into an isotropic part with the subscript I and an anisotropic part with the subscript A. We arrive at

$$\begin{aligned} \Psi^e(\bar{\boldsymbol{C}}, \boldsymbol{M}, \boldsymbol{N}) &= \Psi^e_I(\bar{\boldsymbol{C}}) + \Psi^e_A(\bar{\boldsymbol{C}}, \boldsymbol{M}, \boldsymbol{N}) \\ \Psi^v(\bar{\boldsymbol{C}}, \boldsymbol{M}, \boldsymbol{N}, \boldsymbol{\mathcal{I}}_i, \boldsymbol{\mathcal{A}}_j, \boldsymbol{\mathcal{B}}_k) &= \sum_{i=1}^{n^I_{v,i}} \Psi^v_i(\bar{\boldsymbol{C}}, \boldsymbol{\mathcal{I}}_i) + \sum_{j=1}^{n^A_{v,j}} \Psi^v_j(\bar{\boldsymbol{C}}, \boldsymbol{M}, \boldsymbol{\mathcal{A}}_j) + \sum_{k=1}^{n^A_{v,k}} \Psi^v_k(\bar{\boldsymbol{C}}, \boldsymbol{N}, \boldsymbol{\mathcal{B}}_k)\,. \end{aligned} \tag{88}$$

Observe that the formulation as stated in equation (88) allows the use of a different number of Maxwell-Branches for the isotropic viscoelastic part ($n^I_{v,i}$) as well as for the anisotropic part ($n^A_{v,j}$,$n^A_{v,k}$).

Algorithmic 2nd Piola-Kirchhoff Stresses

Since the general shape of the free energy function is described in the equations above, we derive the isochoric 2^{nd} PIOLA-KIRCHHOFF chain rule stresses $\bar{\boldsymbol{S}}^{iso}$. Again, we drop the superscript *iso* which leads to

$$\begin{aligned} \bar{\boldsymbol{S}} = 2\partial_{\bar{\boldsymbol{C}}}\Psi^{iso} &= \bar{\boldsymbol{S}}^e_I + \bar{\boldsymbol{S}}^e_A + \bar{\boldsymbol{S}}^v_I + \bar{\boldsymbol{S}}^v_A \\ &= 2\partial_{\bar{\boldsymbol{C}}}\Psi^e_I + 2\partial_{\bar{\boldsymbol{C}}}\Psi^e_A + 2\partial_{\bar{\boldsymbol{C}}}\Psi^v_I + 2\partial_{\bar{\boldsymbol{C}}}\Psi^v_A\,, \end{aligned} \tag{89}$$

where

$$\begin{aligned} \bar{\boldsymbol{S}}^v_I &= \sum_{i=1}^{n^I_{v,i}} \bar{\boldsymbol{Q}}^I_i \\ \bar{\boldsymbol{S}}^v_A &= \sum_{j=1}^{n^A_{v,j}} \bar{\boldsymbol{Q}}^A_{a,j} + \sum_{k=1}^{n^A_{v,k}} \bar{\boldsymbol{Q}}^A_{b,k} \end{aligned} \tag{90}$$

 © 2007 Copyright by DYNA*more* GmbH

stand for the isotropic and anisotropic visous overstresses. The evolution equations for the isotropic viscous overstresses are obtained from

$$\dot{\bar{\boldsymbol{Q}}}_i^I + \frac{1}{\tau_i}\bar{\boldsymbol{Q}}_i^I = \beta_i \frac{d}{dt}\left[\hat{\boldsymbol{S}}_I^e\right] , \tag{91}$$

with

$$\hat{\boldsymbol{S}}_I^e := \mathrm{DEV}\left[\bar{\boldsymbol{S}}_I^e\right] = \bar{\boldsymbol{S}}_I^e : \left[\mathbb{I} - \frac{1}{3}\boldsymbol{C}\otimes\boldsymbol{C}^{-1}\right] . \tag{92}$$

Following the same procedure as described in Section 3.1.1, the update equations for the isotropic viscous overstresses read

$$\begin{aligned} \bar{\boldsymbol{Q}}_i^{I,n+1} &= \bar{\boldsymbol{H}}_{\mathcal{I},i}^n + \exp\left\{-\frac{\Delta t}{2\tau_i}\right\}\beta_i\,\hat{\boldsymbol{S}}_I^{e,n+1} \\ \text{with} \quad & \bar{\boldsymbol{H}}_{\mathcal{I},i}^{n+1} = \exp\left\{-\frac{\Delta t}{\tau_i}\right\}\bar{\boldsymbol{Q}}_i^{I,n+1} - \exp\left\{-\frac{\Delta t}{2\tau_i}\right\}\beta_i\,\hat{\boldsymbol{S}}_I^{e,n+1} . \end{aligned} \tag{93}$$

Since we now consider an orthotropic material, we also have to consider the evolution equations for the viscous overstresses associated with the preferred directions $\boldsymbol{a}$ and $\boldsymbol{b}$. Note that the evolution of the stresses in both directions is not coupled explicitly. Therefore, we need to derive seperate evolution equations for both directions. This allows us to employ different relaxation times $\tau_{a,j}$ and $\tau_{b,k}$ for either direction, which may also differ from the isotropic relaxation times τ_i.

First of all, we consider the evolution equation for direction $\boldsymbol{a}$, which is given by

$$\dot{\bar{\boldsymbol{Q}}}_{a,j}^A + \frac{1}{\tau_{a,j}}\bar{\boldsymbol{Q}}_{a,j}^A = \frac{d}{dt}\left[\hat{\boldsymbol{S}}_{\mathcal{A},j}^{v,0}\right] , \tag{94}$$

with

$$\hat{\boldsymbol{S}}_{\mathcal{A},j}^{v,0} := \mathrm{DEV}\left[\bar{\boldsymbol{S}}_{\mathcal{A},j}^{v,0}\right] = \bar{\boldsymbol{S}}_{\mathcal{A},j}^{v,0} : \left[\mathbb{I} - \frac{1}{3}\boldsymbol{C}\otimes\boldsymbol{C}^{-1}\right] . \tag{95}$$

In this case the update equation reads

$$\begin{aligned} \bar{\boldsymbol{Q}}_{a,j}^{A,n+1} &= \bar{\boldsymbol{H}}_{\mathcal{A},j}^n + \exp\left\{-\frac{\Delta t}{2\tau_{a,j}}\right\}\hat{\boldsymbol{S}}_{\mathcal{A},j}^{v,0,n+1} \\ \text{with} \quad & \bar{\boldsymbol{H}}_{\mathcal{A},j}^{n+1} = \exp\left\{-\frac{\Delta t}{\tau_{a,j}}\right\}\bar{\boldsymbol{Q}}_{a,j}^{A,n+1} - \exp\left\{-\frac{\Delta t}{2\tau_{a,j}}\right\}\hat{\boldsymbol{S}}_{\mathcal{A},j}^{v,0,n+1} . \end{aligned} \tag{96}$$

The same procedure is applied to direction $\boldsymbol{b}$, which yields the evolution equation

$$\dot{\bar{\boldsymbol{Q}}}_{b,k}^A + \frac{1}{\tau_{b,k}}\bar{\boldsymbol{Q}}_{b,k}^A = \frac{d}{dt}\left[\hat{\boldsymbol{S}}_{\mathcal{B},k}^{v,0}\right] , \tag{97}$$

with

$$\hat{\boldsymbol{S}}_{\mathcal{B},k}^{v,0} := \mathrm{DEV}\left[\bar{\boldsymbol{S}}_{\mathcal{B},k}^{v,0}\right] = \bar{\boldsymbol{S}}_{\mathcal{B},k}^{v,0} : \left[\mathbb{I} - \frac{1}{3}\boldsymbol{C}\otimes\boldsymbol{C}^{-1}\right] . \tag{98}$$

© 2007 Copyright by DYNA*more* GmbH

Finally, the update equation is defined by

$$\bar{\boldsymbol{Q}}^{A,n+1}_{b,k} = \bar{\boldsymbol{H}}^{n}_{\mathcal{B},k} + \exp\left\{-\frac{\Delta t}{2\tau_{b,k}}\right\} \hat{\boldsymbol{S}}^{v,0,n+1}_{\mathcal{B},k}$$

$$\text{with} \quad \bar{\boldsymbol{H}}^{n+1}_{\mathcal{B},k} = \exp\left\{-\frac{\Delta t}{\tau_{b,k}}\right\} \bar{\boldsymbol{Q}}^{A,n+1}_{b,k} - \exp\left\{-\frac{\Delta t}{2\tau_{b,k}}\right\} \hat{\boldsymbol{S}}^{v,0,n+1}_{\mathcal{B},k} \,. \tag{99}$$

In the equations above $\hat{\boldsymbol{S}}^{v,0}_{\mathcal{A},j}$ and $\hat{\boldsymbol{S}}^{v,0}_{\mathcal{B},k}$ are the instantaneous deviatoric viscous overstresses for the directions $\boldsymbol{a}$ and $\boldsymbol{b}$. Instantaneous means that the strain-like internal variables are held constant when performing the derivative. The quantities $\bar{\boldsymbol{H}}^{n+1}_{\mathcal{I},i}$, $\bar{\boldsymbol{H}}^{n+1}_{\mathcal{A},j}$ and $\bar{\boldsymbol{H}}^{n+1}_{\mathcal{B},k}$ are the history variables, which need to be stored in every time step. With all the terms at hand, the isochoric chain rule stresses at time t_{n+1} may be computed according to

$$\bar{\boldsymbol{S}}^{n+1} = \bar{\boldsymbol{S}}^{n+1}_{I} + \bar{\boldsymbol{S}}^{n+1}_{A} \,, \tag{100}$$

with

$$\bar{\boldsymbol{S}}^{n+1}_{I} = \left[1 + \sum_{i=1}^{n^I_v} \beta_i \exp\left\{-\frac{\Delta t}{2\tau_i}\right\}\right] \bar{\boldsymbol{S}}^{e,n+1}_{I} + \sum_{j=1}^{n^I_v} \bar{\boldsymbol{H}}^{n}_{\mathcal{I},i} \tag{101}$$

and

$$\begin{aligned} \bar{\boldsymbol{S}}^{n+1}_{A} &= \bar{\boldsymbol{S}}^{e,n+1}_{A} + \sum_{j=1}^{n^A_{v,j}} \bar{\boldsymbol{Q}}^{A}_{a,j} + \sum_{k=1}^{n^A_{v,k}} \bar{\boldsymbol{Q}}^{A}_{b,k} \\ &= \bar{\boldsymbol{S}}^{e,n+1}_{A} + \sum_{j=1}^{n^A_{v,j}} \exp\left\{-\frac{\Delta t}{2\tau_{a,j}}\right\} \bar{\boldsymbol{S}}^{v,0,n+1}_{\mathcal{A},j} + \sum_{j=1}^{n^A_{v,j}} \bar{\boldsymbol{H}}^{n}_{\mathcal{A},j} \\ &\quad + \sum_{k=1}^{n^A_{v,k}} \exp\left\{-\frac{\Delta t}{2\tau_{b,k}}\right\} \bar{\boldsymbol{S}}^{v,0,n+1}_{\mathcal{B},k} + \sum_{k=1}^{n^A_{v,k}} \bar{\boldsymbol{H}}^{n}_{\mathcal{B},k} \,. \end{aligned} \tag{102}$$

Algorithmic Lagrangian Moduli

The Lagrangian isochoric chain rule moduli are derived according to

$$\bar{\mathbb{C}}^{iso} = 2\partial_{\bar{\boldsymbol{C}}} \bar{\boldsymbol{S}}^{iso} \,.$$

Here, they have the form

$$\begin{aligned} \bar{\mathbb{C}}^{n+1}_{iso} &= \left[1 + \sum_{i=1}^{n^I_v} \beta_i \exp\left\{-\frac{\Delta t}{2\tau_i}\right\}\right] \bar{\mathbb{C}}^{e,n+1}_{I} + \bar{\mathbb{C}}^{e,n+1}_{A} \\ &+ \sum_{j=1}^{n^A_{v,j}} \exp\left\{-\frac{\Delta t}{2\tau_{a,j}}\right\} \bar{\mathbb{C}}^{v,0,n+1}_{\mathcal{A},j} + \sum_{k=1}^{n^A_{v,k}} \exp\left\{-\frac{\Delta t}{2\tau_{b,k}}\right\} \bar{\mathbb{C}}^{v,0,n+1}_{\mathcal{B},k} \end{aligned} \tag{103}$$

© 2007 Copyright by DYNA*more* GmbH

4.4.1. Free Energy Function of the Orthotropic Linear Viscoelastic Model

Now, we define a specific free energy function enabling the describtion orthotropic finite linear viscoelastic behaviour. According to (88), we need the following terms

$$
\begin{aligned}
\Psi_I^e &= C_{10}(\bar{I}_1 - 3) + C_{20}(\bar{I}_1 - 3)^2 + C_{30}(\bar{I}_1 - 3)^3 \\
\Psi_A^e &= \alpha_{e1}(\bar{J}_4 - 1)^2 + \alpha_{e2}\left[(\bar{J}_5 - 1) - (\bar{I}_1 - 3)(\bar{J}_4 - 1) + (\bar{I}_2 - 3) - 2(\bar{J}_4 - 1)\right] \\
&+ \alpha_{e3}(\bar{J}_6 - 1)^2 + \alpha_{e4}\left[(\bar{J}_7 - 1) - (\bar{I}_1 - 3)(\bar{J}_6 - 1) + (\bar{I}_2 - 3) - 2(\bar{J}_6 - 1)\right] \\
\Psi_{I,i}^v &= \beta_i \Psi_I^e \\
\Psi_{A,i}^v &= \alpha_{v1,i}(\bar{J}_4 - 1)^2 + \alpha_{v2,i}\left[(\bar{J}_5 - 1) - (\bar{I}_1 - 3)(\bar{J}_4 - 1) + (\bar{I}_2 - 3) - 2(\bar{J}_4 - 1)\right] \\
&+ \alpha_{v3,i}(\bar{J}_6 - 1)^2 + \alpha_{v4,i}\left[(\bar{J}_7 - 1) - (\bar{I}_1 - 3)(\bar{J}_6 - 1) + (\bar{I}_2 - 3) - 2(\bar{J}_6 - 1)\right] .
\end{aligned}
\tag{104}
$$

The invariants are defined in (70) and (71). Again, we assume the coupling $\Psi_{I,i}^v = \beta_i \Psi_I^e$ between the isotropic viscous part of the free energy with the isotropic elastic part for every Maxwell-Branch. Ψ_A^e and $\Psi_{A,i}^v$ include the free energy terms correlated with the preferred directions $\boldsymbol{a}$ and $\boldsymbol{b}$. The model is implemented making use of four Maxwell-Branches for the overall viscous contribution. The material parameters are summarized in the table below.

	Isotropic	Anisotropic	Total
Elasticity Parameters	κ,C_{10},C_{20},C_{30}	α_{e1}, α_{e2}, α_{e3}, α_{e4}	8
Viscosity Parameters (i=1,2,3,4)	β_i,τ_i	$\alpha_{v1,i}$,$\alpha_{v2,i}$,$\tau_{a,i}$ $\alpha_{v3,i}$,$\alpha_{v4,i}$,$\tau_{b,i}$	32

Table 1: Material parameters of orthotropic linear viscoelasticity model

According to the equations (101) and (102), we need a formulation for $\bar{\boldsymbol{S}}_I^e$, which is already given in equation (28)

$$\bar{\boldsymbol{S}}^{iso} = 2\left[C_{10} + 2C_{20}(\bar{I}_1 - 3) + 3C_{30}(\bar{I}_1 - 3)^2\right]\mathbf{1} .$$

The anisotropic elastic contribution $\bar{\boldsymbol{S}}_A^e$ is defined in (81)

$$\bar{\boldsymbol{S}}^{iso} = f_1\,\mathbf{1} + f_2\,\bar{\boldsymbol{C}} + f_3\,\boldsymbol{M} + f_4\,(\boldsymbol{M}\bar{\boldsymbol{C}} + \bar{\boldsymbol{C}}\boldsymbol{M}) + f_5\,\boldsymbol{N} + f_6\,(\boldsymbol{N}\bar{\boldsymbol{C}} + \bar{\boldsymbol{C}}\boldsymbol{N}) ,$$

with

$$
\begin{aligned}
f_1 &= 2C_{10} + 4C_{20}(\bar{I}_3 - 3) + 6C_{30}(\bar{I}_3 - 3)^2 \\
&\quad +2(\alpha_{e2} + \alpha_{e4})\bar{I}_1 - 2(\alpha_{e2}(\bar{J}_4 - 1) + \alpha_{e4}(\bar{J}_6 - 1)) \\
f_2 &= -2(\alpha_{e2} + \alpha_{e4}) \\
f_3 &= 4\alpha_{e1}(\bar{J}_4 - 1) - 2\alpha_{e2}(\bar{I}_1 - 3) - 4\alpha_{e2} \\
f_4 &= 2\alpha_{e2} = \text{const.} \\
f_5 &= 4\alpha_{e3}(\bar{J}_6 - 1) - 2\alpha_{e4}(\bar{I}_1 - 3) - 4\alpha_{e4} \\
f_6 &= 2\alpha_{e4} = \text{const.} ,
\end{aligned}
$$

the equation for the viscous stresses $\bar{\boldsymbol{S}}^{v,0}_{\mathcal{A},j}$ in $\boldsymbol{a}$-direction is given by

$$\begin{aligned}\bar{\boldsymbol{S}}^{v,0}_{\mathcal{A},j} &= \left[2\alpha_{v2,j}\bar{I}_1 - 2\alpha_{v2,j}(\bar{J}_4 - 1)\right] \boldsymbol{1} \\ &- 2\alpha_{v2,j}\,\bar{\boldsymbol{C}} \\ &+ \left[4\alpha_{v1,j}(\bar{J}_4 - 1) - 2\alpha_{v2,j}(\bar{I}_1 - 3) - 4\alpha_{v2,j}\right] \boldsymbol{M} \\ &+ 2\alpha_{v2,j}\,(\boldsymbol{M}\bar{\boldsymbol{C}} + \bar{\boldsymbol{C}}\boldsymbol{M}) \end{aligned} \tag{105}$$

and the equation for the viscous stresses $\bar{\boldsymbol{S}}^{v,0}_{\mathcal{B},k}$ in $\boldsymbol{b}$-direction read

$$\begin{aligned}\bar{\boldsymbol{S}}^{v,0}_{\mathcal{B},k} &= \left[2\alpha_{v4,k}\bar{I}_1 - 2\alpha_{v4,k}(\bar{J}_6 - 1)\right] \boldsymbol{1} \\ &- 2\alpha_{v4,k}\,\bar{\boldsymbol{C}} \\ &+ \left[4\alpha_{v3,k}(\bar{J}_6 - 1) - 2\alpha_{v4,j}(\bar{I}_1 - 3) - 4\alpha_{v4,k}\right] \boldsymbol{N} \\ &+ 2\alpha_{v4,k}\,(\boldsymbol{N}\bar{\boldsymbol{C}} + \bar{\boldsymbol{C}}\boldsymbol{N})\,. \end{aligned} \tag{106}$$

The equations for the isotropic elastic chain rule moduli $\bar{\mathbb{C}}^e_I$ are obtained as

$$\bar{\mathbb{C}}^e_I = \left[8C_{20} + 24C_{30}(\bar{I}_3 - 3)\right] \boldsymbol{1} \otimes \boldsymbol{1}\,, \tag{107}$$

whereas the anisotropic elastic contribution $\bar{\mathbb{C}}^e_A$ is given by

$$\begin{aligned}\bar{\mathbb{C}}^e_A &= 4(\alpha_{e2} + \alpha_{e4})\,\boldsymbol{1} \otimes \boldsymbol{1} \\ &- 4\alpha_{e2}\,(\boldsymbol{M} \otimes \boldsymbol{1} + \boldsymbol{1} \otimes \boldsymbol{M}) \\ &+ 8\alpha_{e1}\,\boldsymbol{M} \otimes \boldsymbol{M} \\ &+ 4\alpha_{e2}\,(\boldsymbol{M}\tilde{\otimes}\boldsymbol{1} + \boldsymbol{1}\tilde{\otimes}\boldsymbol{M}) \\ &- 4(\alpha_{e2} + \alpha_{e4})\,\mathbb{I} \\ &- 4\alpha_{e4}\,(\boldsymbol{N} \otimes \boldsymbol{1} + \boldsymbol{1} \otimes \boldsymbol{N}) \\ &+ 8\alpha_{e3}\,\boldsymbol{N} \otimes \boldsymbol{N} \\ &+ 4\alpha_{e4}\,(\boldsymbol{N}\tilde{\otimes}\boldsymbol{1} + \boldsymbol{1}\tilde{\otimes}\boldsymbol{N})\,. \end{aligned} \tag{108}$$

For the viscous Lagrangian moduli for direction $\boldsymbol{a}$ we get

$$\begin{aligned}\bar{\mathbb{C}}^{v,0}_{\mathcal{A},j} &= 4\alpha_{v2,j}\,\boldsymbol{1} \otimes \boldsymbol{1} \\ &- 4\alpha_{v2,j}\,(\boldsymbol{M} \otimes \boldsymbol{1} + \boldsymbol{1} \otimes \boldsymbol{M}) \\ &+ 8\alpha_{v1,j}\,\boldsymbol{M} \otimes \boldsymbol{M} \\ &+ 4\alpha_{v2,j}\,(\boldsymbol{M}\tilde{\otimes}\boldsymbol{1} + \boldsymbol{1}\tilde{\otimes}\boldsymbol{M}) \\ &- 4\alpha_{v2,j}\,\mathbb{I} \end{aligned} \tag{109}$$

and for the counterpart, i.e. for direction $\boldsymbol{b}$, we end up with

$$\begin{aligned}\bar{\mathbb{C}}^{v,0}_{\mathcal{B},k} &= 4\alpha_{v4,k}\,\boldsymbol{1} \otimes \boldsymbol{1} \\ &- 4\alpha_{v4,k}\,(\boldsymbol{N} \otimes \boldsymbol{1} + \boldsymbol{1} \otimes \boldsymbol{N}) \\ &+ 8\alpha_{v3,k}\,\boldsymbol{N} \otimes \boldsymbol{N} \\ &+ 4\alpha_{v4,k}\,(\boldsymbol{N}\tilde{\otimes}\boldsymbol{1} + \boldsymbol{1}\tilde{\otimes}\boldsymbol{N}) \\ &- 4\alpha_{v4,k}\,\mathbb{I}\,. \end{aligned} \tag{110}$$

© 2007 Copyright by DYNA*more* GmbH

With the insertion of these relations into equation (89) and (103), the constitutive equations for the numerical implementation are complete.

5. Numerical Examples

The material model was implemented into the finite element code LS-DYNA. Thereby, an explicit and an implicit implementation has been carried out. To show the performance of the model and display anisotropy effects, we use the tranversely isotropic model setting $\alpha_{e3} = \alpha_{e4} = 0$. Also, the relaxation times are set equal for the isotropic and anisotropic viscous part. First of all, in the framework of the explicit implementation we examine a tensile test of a fiber-reinforced bar and the inflation of a fiber-reinforced circular membrane. The last example compares the explicit implementation to the implicit implementation using a uniaxial single element tensile test. Note that the material paramaters are intentionally chosen in order to demonstrate the effects clearly.

5.1. Numerical Example: Tensile Test of a Fiber-Reinforced Bar

In the first example we demonstrate the effects of the structural tensor $\boldsymbol{M} = \boldsymbol{a} \otimes \boldsymbol{a}$ for transverse isotropy. To this end, we consider a rectangular bar composed of two layers of fiber-reinforced incompressible rubber-like material with two different fiber-orientations in both layers. It is clamped in the yz-plane at $x = 0$ mm. The dimensions of the bar are 100 × 50 × 20 mm. For the upper layer we define an in-plane fiber orientation of φ_u = -45°, whereas the in-plane fiber orientation in the lower layer is φ_l = 45°. The bar is elongated in x-direction up to 250 mm. Thereby, the maximum stretch-rate is $\dot{\lambda} = 75\frac{1}{s}$. This stretch-rate is chosen to examine the robustness of the model for applications with high stretch rates, for example crash-simulations. The loadcurve u_x applied to the nodes in plane $x = 100$ mm is shown in Figure 2.

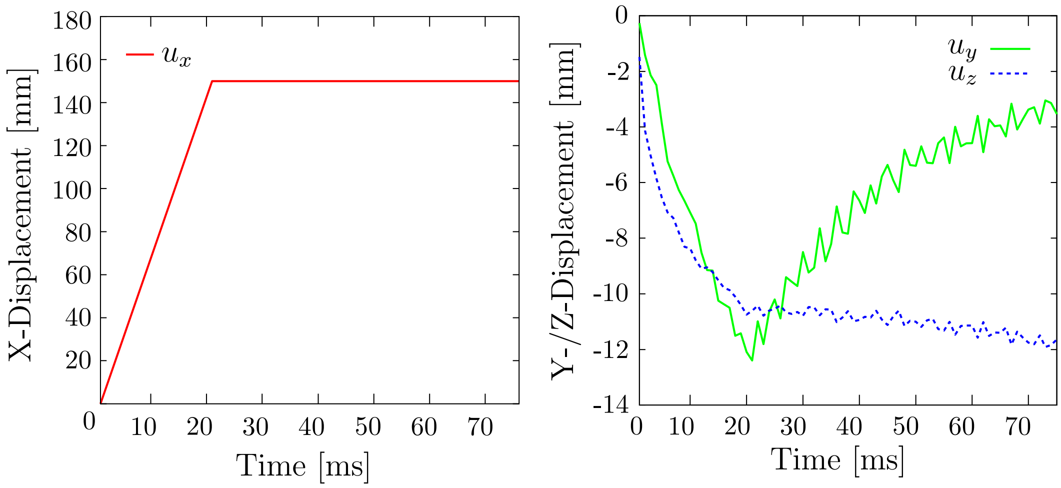

Figure 2: Displacement curves of point A during the relaxation test

The bar is discretisized with 800 constant stress solid elements (ETYP=1 in LS-DYNA) using a default hourglass control (IHQ=6).The material parameters for the assumed quasi-incompressible material are given in the table below.

	Isotropic				Anisotropic			
Elastic	κ	C_{10}	C_{20}	C_{30}	α_{e1}		α_{e2}	
$[kN/mm^2]$	10.00	$2.947 \cdot 10^{-4}$	$-3.01 \cdot 10^{-5}$	$5.605 \cdot 10^{-6}$	0.001		0.002	
Viscoelastic	β_1	τ_1	β_2	τ_2	$\alpha_{v1,1}$	$\alpha_{v1,2}$	$\alpha_{v2,1}$	$\alpha_{v2,2}$
$[kN/mm^2]$	0.200	100.000	0.30	10.00	0.011	0.021	0.012	0.022

Table 2: Material parameters for tensile test of fiber-reinforced bar

The parameters were set such that the anisotropy effects are pointed out clearly. The deformed shape of the bar depends strongly on the orientation of the structural tensor $\boldsymbol{M}$. As the bar is elongated in a deformation controlled process, torsion of the bar will occur due to the embedded fibers, which can be seen in Figure 3.

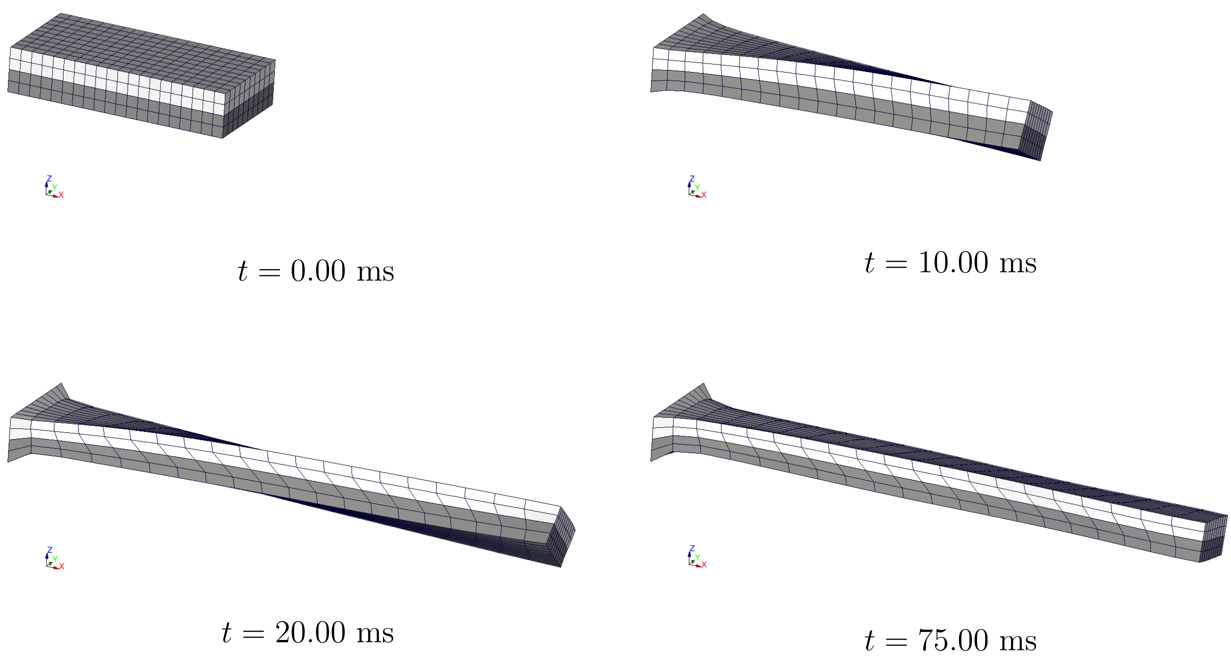

Figure 3: Deformation of a rectangular bar during relaxation test

This phenomenon is known from the deformation of fiber-reinforced composite laminates. The rotation is such that the orientations of the fibers allign with the loading axis because the stiffness of the material rises to its peak in fiber direction. Since we consider transversely isotropic linear viscoelasticity, the behaviour during the relaxation phase is of great interest. In Figure 3 and in Figure 4, this behaviour is outlined impressively.

© 2007 Copyright by DYNA*more* GmbH

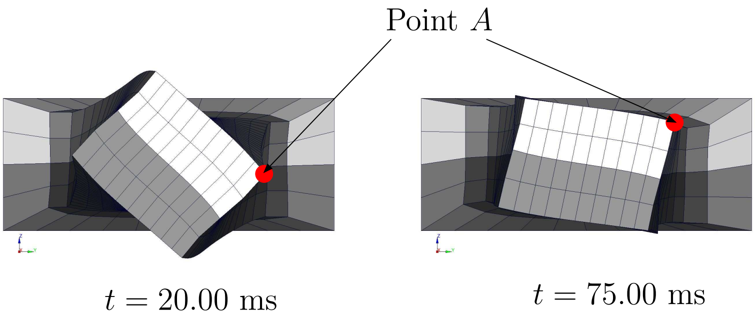

Figure 4: Visualization of relaxation process

Comparing the pictures in Figure 4 we observe that the bar rotates backwards between the beginning of the relaxation phase at time $t = 20.00$ms and the end of the simulation at time $t = 75.00$ms, until the viscous overstresses have decayed. This may also be seen in the y-displacement curve for the node at Point A in Figure 2b. The maximum deflection occurs at the beginning of the relaxation period and it decreases as time advances. Since the fibers are located in the xy-plane, there is no relaxation in z-direction.

5.2. Numerical Example: Inflation of a Fibre-reinforced Circular Membrane

In the second example we simulate the inflation of a fiber-reinforced circular membrane with an in-plane fiber direction of $\varphi = 45°$. The membrane consists of one layer of fiber-reinforced rubber and its radius is $400mm$, whereas the thickness is $20mm$. The pressure rises linearly up to a maximum pressure of $p = 0.012\, kN/mm^2$ after $t = 50ms$. The translational degrees of freedom of the nodes on the circumference of the lower surface of the membrane are fixed in all directions and the mebrane is discretisized with a layer of constant stress solid elements (ETYP=1 in LS-DYNA) and a layer of Belytschko-Tsay (ETYP=2 in LS-DYNA) shell elements with the thickness of $2mm$, which are necessary for the application of the pressure. We use the same hourglass control as in Section 5.1. The constitutive model is the same as for the bar considered in Section 5.1, but this time we investigate two settings. The first one is an isotropic elastic setting and the other one is an anisotropic elastic setting. The material parameters are listed in the table below. Note that for the isotropic elastic case α_{e1} and α_{e2} are set to zero.

	Isotropic				Anisotropic	
Elastic	κ	C_{10}	C_{20}	C_{30}	α_{e1}	α_{e2}
$[kN/mm^2]$	10.00	$2.257 \cdot 10^{-3}$	$-3.33 \cdot 10^{-5}$	$3.518 \cdot 10^{-9}$	0.01	0.02

Table 3: Material parameters for inflation of fiber-reinforced circular membrane

In Figure 5 different stages of the deformation are depicted for the isotropic elastic and transversely isotropic case.

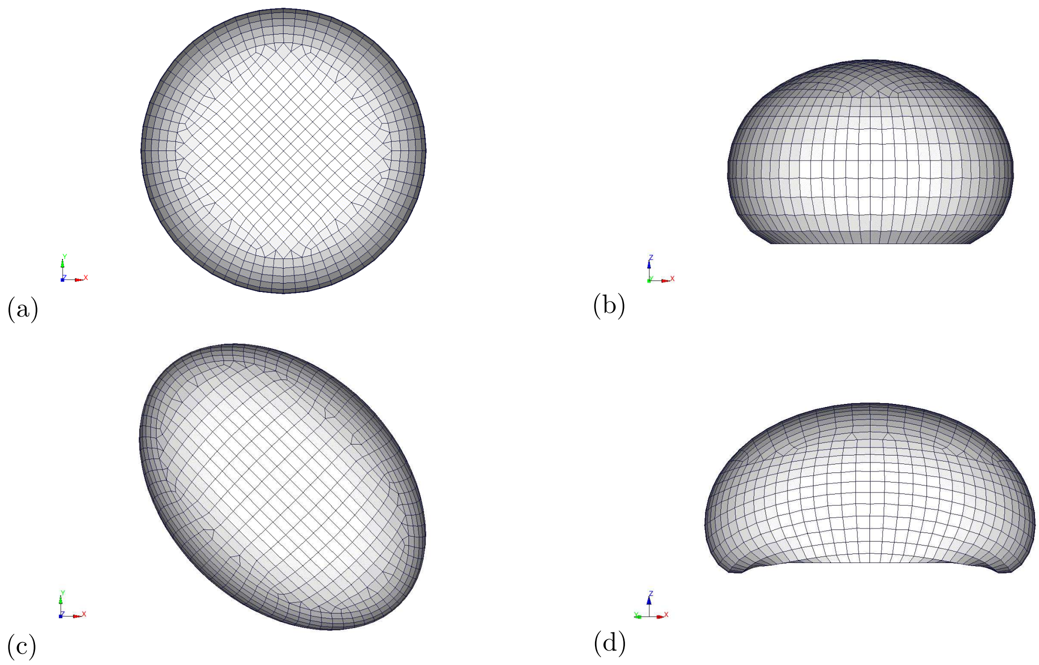

Figure 5: Isotropic elasticity (a) top view (b) side view ; Transversely isotropic elasticity (c) top view (d) side view

Observe that for the isotropic elastic deformation the deformed membrane takes a sphere-like shape, whereas for the anisotropic elastic case it displays an ellipsoidal shape with two of the principal axes alligned in fiber direction and transverse to it. Since the stiff fibers have an orientation of $\varphi = 45°$ in the xy-plane, the extension coaxial to the fiber direction is less than in perpendicular directions.

5.3. Numerical Example: Single Element Tensile Test

The material model is implemented into LS-DYNA in the sense of an explicit and an implicit implementation. In order to discuss the transversely isotropic linear visoelastic material behaviour and also for the comparison of the explicit and implicit formulation, we consider a single element relaxation test in this example (see Figure 6).

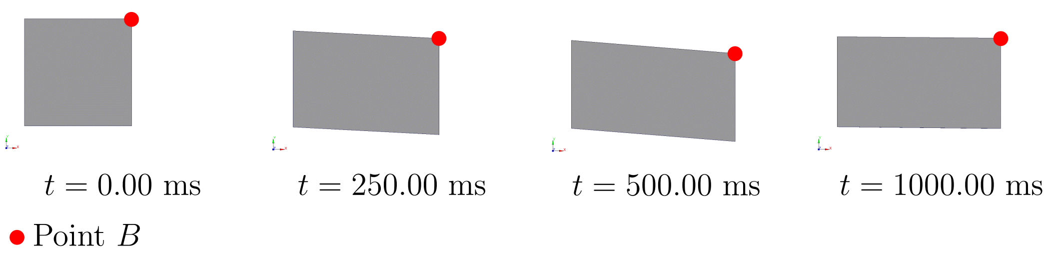

Figure 6: Single element relaxation test

 © 2007 Copyright by DYNA*more* GmbH

The fully integrated solid element with edge lenghts $10mm$ is deformed in x-direction in a displacement controlled deformation process according to the loadcurve depicted in Figure 7a. The in-plane fiber orientation is $\varphi = 45°$ and the maximum elongation of the element is $5mm$ at time $t = 500ms$.

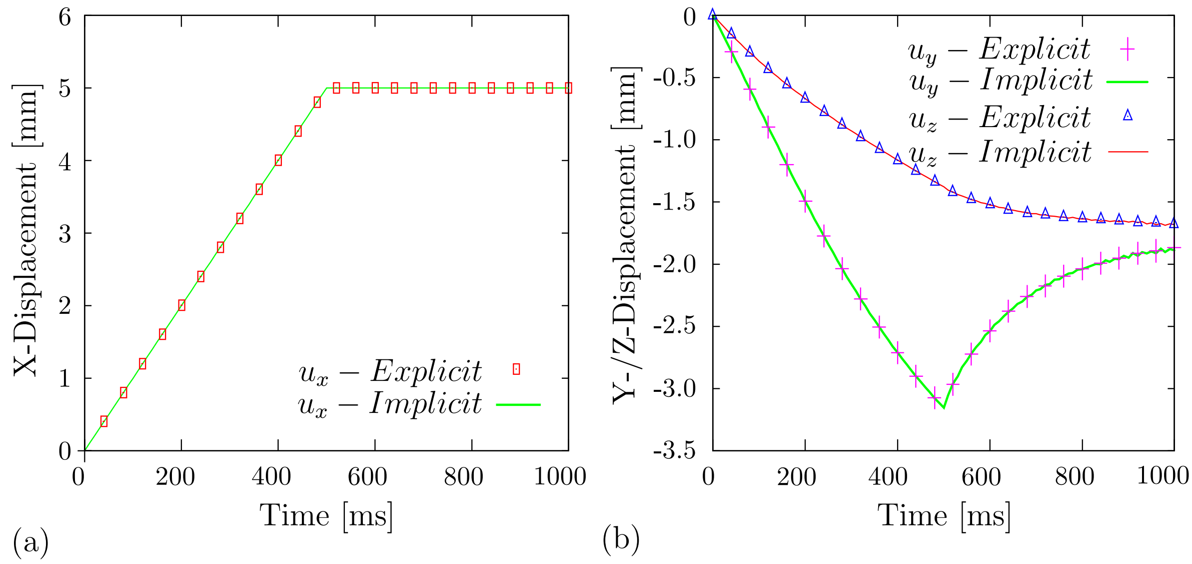

Figure 7: Displacement curves of point B during the relaxation test

As expected, the displacement curves for the explicit and imlicit implementation shown in Figure 7 coincide for the x-, y- and z-displacement. Again, the curve for the y-displacement depicted in Figure 7b shows the relaxation of the material clearly, while there is no relaxation in z-direction. The material parameters used for the simulation of the single element relaxation test are listed in the table below.

	Isotropic				Anisotropic			
Elastic	κ	C_{10}	C_{20}	C_{30}	α_{e1}		α_{e2}	
$[kN/mm^2]$	10.00	$2.947 \cdot 10^{-4}$	$-3.01 \cdot 10^{-5}$	$5.605 \cdot 10^{-6}$	0.01		0.02	
Viscoelastic	β_1	τ_1	β_2	τ_2	$\alpha_{v1,1}$	$\alpha_{v1,2}$	$\alpha_{v2,1}$	$\alpha_{v2,2}$
$[kN/mm^2]$	0.50	100.000	0.70	10.00	1.11	1.12	1.11	1.12

Table 4: Material parameters for single element tensile test

The stress state inside the element can be seen in Figure 8a. Since the displacement u_x is prescribed, stresses only evolve in x-direction. All other components of the Cauchy stresses are zero due to the equilibrium conditions. Comparing the stress response evaluated in an explicit and an implicit simulation we again find no difference in the curves displayed in Figure 8b, which we expect for a single element test.

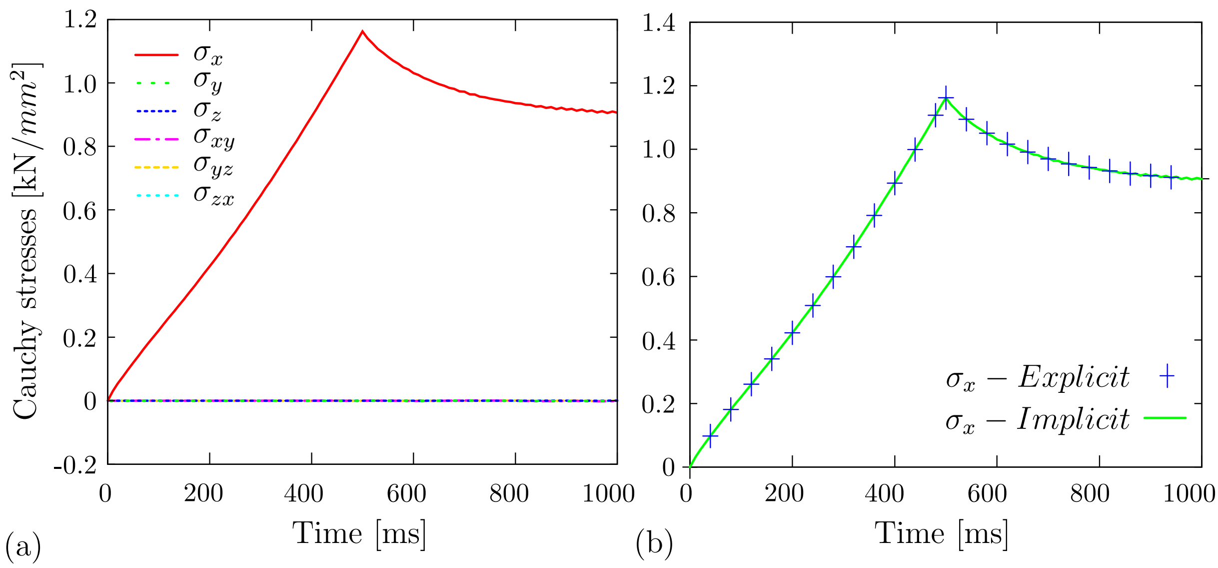

Figure 8: Cauchy stresses (a) Stress state in implicit simulation (b) Comparison with explicit simulation

6. Conclusion

In this article we proposed a polyconvex free energy function capable of describing orthotropic and transversely isotropic linear viscoelastic material behaviour at finite deformations. The model has been implemented into LS-DYNA enabling explicit and implicit finite element simulations of representative boundary value problems. Through the simulations, we outlined that the model mirrors the expected results in a qualitative manner. The model is also very versatile because with a specific choice of the material parameters it is possible to describe isotropic elastic or linear viscoelastic material behaviour as well as an anisotropic elastic or linear viscoelsatic material response.

In a further step, the performance of the model will be evaluated in comparison to experimental data, which is necessary for making quantitative judgments about the model's capabilites.

Acknowledgment

This article was written in the course of a cooperation between the *DaimlerChrysler AG* and the *Institute of Applied Mechanics (Chair 1)* of the *University of Stuttgart*. There it was supervised by Prof. Dr.-Ing. Christian Miehe and Serdar Göktepe, M.Sc. The authors would like to thank both of them for making this work possible and for the excellent supervision during the last couple of months.

 © 2007 Copyright by DYNA*more* GmbH

References

[1] APEL, N. [2004]: *"Approaches to the Description of Anisotropic Material Behaviour at Finite Elastic and Plastic Deformations - Theory and Numerics"*. Ph.D. Thesis, Institut für Mechanik im Bauwesen, Lehrstuhl I, Universität Stuttgart.

[2] BOEHLER, J. P. (EDITOR) [1987]: *"Applications of Tensor Functions in Solid Mechanics"*. Springer-Verlag, Wien, CISM Courses and Lectures No. 292.

[3] CHRISTENSEN, R. M. [2003]: *"Theory of Viscoelasticity: An Introduction"*. Dover Publications Inc., Mineola, New York.

[4] GOVINDJEE, S. [1991]: *"Physical and Numerical Modelling in Filled Elastomeric Systems"*. Ph.D. Thesis, Order Number 9206770, Stanford University.

[5] HOLZAPFEL, G. A.; GASSER, C. G. [2000]: *"A Viscoelastic Model for Fiber-Reinforced Composites at Finite Strains: Continuum Basis, Computational Aspects and Applications"*. Computer Methods in Applied Mechanics and Engineering, Vol. 190: 4379–4403.

[6] KALISKE, M.; ROTHERT, H. [1997]: *"Formulation and Implementation of Three-Dimensional Viscoelasticity at Small and Finite Strains"*. Computational Mechanics, Vol. 19: 228–239.

[7] MALVERN, L. E. [1969]: *"Introduction to the Mechanics of a Continuous Medium"*. Prentice-Hall Inc., New Jersey.

[8] MARSDEN, J. E.; HUGHES, T. J. R. [1994]: *"Mathematical Foundations of Elasticity"*. Dover Publications Inc., Mineola, New York.

[9] MIEHE, C. [1994]: *"Aspects of the Formulation and Finite Element Implementation of Large Strain Isotropic Elasticity"*. International Journal for Numerical Methods in Engineering, Vol. 37: 1981–2004.

[10] OGDEN, R. W. [1972]: *"Large Deformation Isotropic Elastictiy - On the Correlation of Theory and Experiment for Incompressible Rubberlike Solids"*. Proceedings of the Royal Society London A, 326: 565–584.

[11] RIEGER, S. [2004]: *"Temperaturabhängige Beschreibung visko-elasto-plastischer Deformationen kurzglasfaserverstärkter Thermoplaste: Modellbildung, Numerik und Experimente"*. Ph.D. Thesis, Institut für Mechanik im Bauwesen, Lehrstuhl I, Universität Stuttgart.

[12] SCHRÖDER, J. [1996]: *"Theoretische und algorithmische Konzepte zur phänomenologischen Beschreibung anisotropen Materialverhaltens"*. Ph.D. Thesis, Institut für Mechanik im Bauwesen, Lehrstuhl I, Universität Stuttgart, Bericht Nr.: I-1 (1996) - Nachdruck.

[13] SCHRÖDER, J.; NEFF, P. [2002]: *"Invariant Formulation of Hyperelastic Transverse Isotropy Based on Polyconvex Free Energy Functions"*. International Journal of Solids and Structures, Vol.40: 401–445.

© 2007 Copyright by DYNA*more* GmbH

[14] Simo, J. C. [1987]: *"On a Fully Three-dimensional Finite-Strain Viscoelastic Damage Model: Formulation and Computational Aspects"*. Computer Methods in Applied Mechanics and Engineering, Vol.60: 153–173.

[15] Simo, J. C.; Taylor, R. L. [1982]: *"Penalty function formulations for incompressible nonlinear elastostatics"*. Computer Methods in Applied Mechanics and Engineering, Vol. 35: 107–118.

[16] Simo, J. C.; Hughes, T. J. R. [2000]: *"Computational Inelasticity"*. Springer-Verlag, Berlin.

[17] Spencer, A. J. M. [1971]: *"Theory of Invariants"*. in: Eringen, Continuum Physics Volume 1, Academic Press, New York.

[18] Spencer, A. J. M. [1987]: *"Isotropic Polynomial Invariants and Tensor Functions"*. in: Boehler, Application of Tensor Functions in Solid Mechanics, Springer-Verlag, Wien, CISM Courses and Lectures No. 292.

[19] Treloar, L. R. G. [1944]: *"Stress–Strain Data for Vulcanised Rubber Under Various Types of Deformation"*. Transactions of the Faraday Society, Vol.40: 59–70.

[20] Truesdell, C.; Noll, W. [1960]: *"The Nonlinear Field Theories of Mechanics", Handbuch der Physik Bd. III/3, Edited by S. Flügge.* Springer-Verlag, Berlin.

[21] Yeoh, O. H. [1990]: *"Characterization of Elastic Properties of Carbon-black-filled Rubber Vulcanizates"*. Rubber Chemistry and Technology, Vol. 63: 792–805.

 © 2007 Copyright by DYNA*more* GmbH